DOI: 10.2169/internalmedicine.46.0117

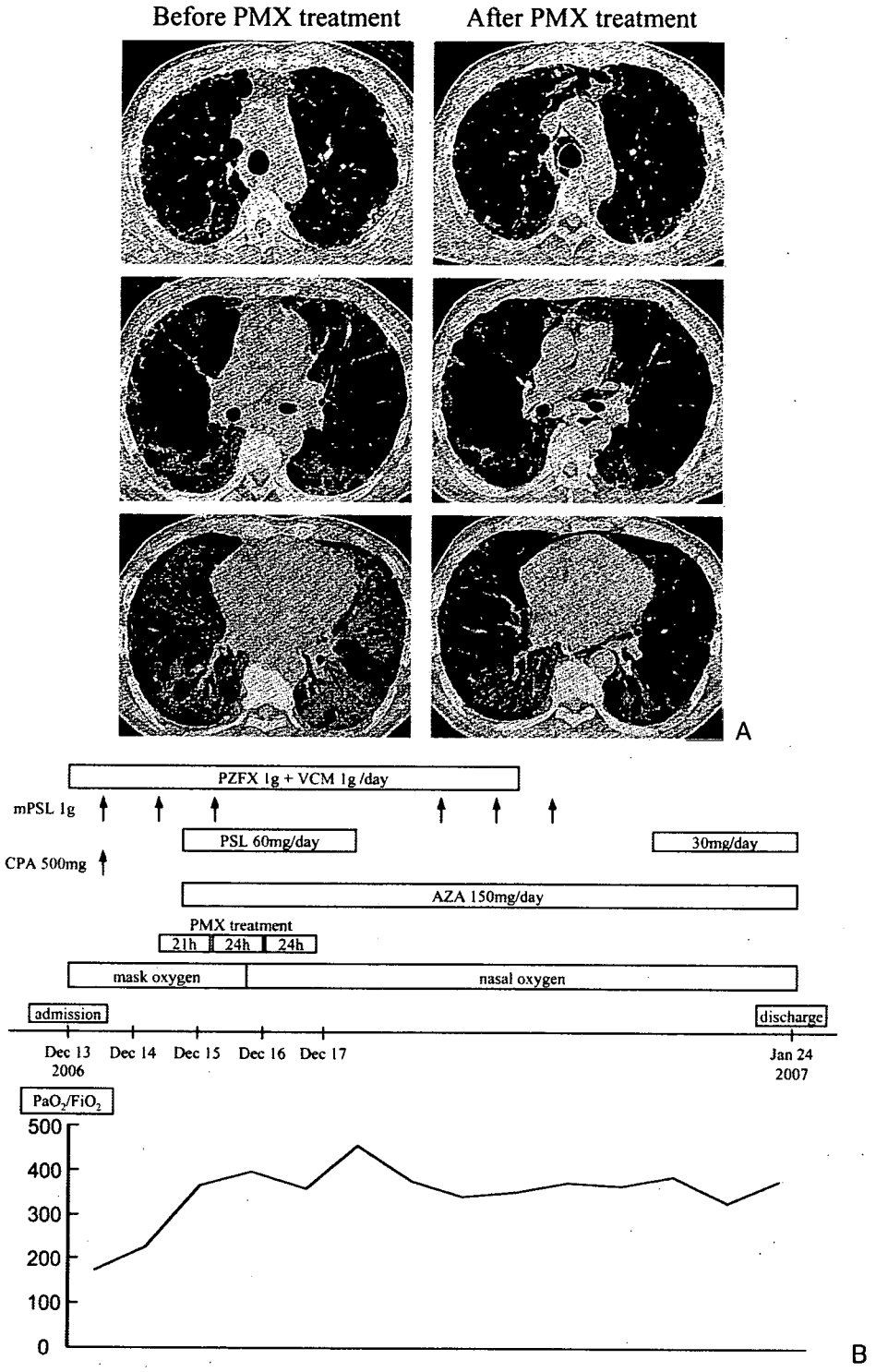

Figure 2. A: Chest HRCT before and after the PMX hemoperfusion treatment of Case 2. Chest HRCT showed improvement of the ground-glass opacity. B: Clinical course of Case 2.

moperfusion treatment (Toraymixin 20R, Toray Medical Co., Tokyo, Japan, at a flow rate of 80 ml/min). Nafamostat mesilate (Torii Pharma Co., Tokyo, Japan) was used as an anticoagulant during the PMX hemoperfusion treatment. We performed PMX hemoperfusion treatment 3 times (20 hours, 24 hours and 24 hours). After PMX hemoperfusion treatment, P/F ratio improved from 225.0 to 395.6. Chest HRCT showed improvement of the ground-glass opacity (Fig. 2A). The laboratory findings at this point were as follows: LDH 221 IU/L; CRP 0.32 mg/dl; KL-6 748 U/mL; endotoxin and β-D glucan were under detectable concentration. BALF examination after PMX hemoperfusion treatment showed decreased total cell counts and an increase of neutrophil percentage. Prednisolone (30 mg/day) and azathioprine (150 mg/day) was administered orally as maintenance therapy. His symptoms improved and he was discharged 44 days af-

DOI: 10.2169/internalmedicine.46.0117

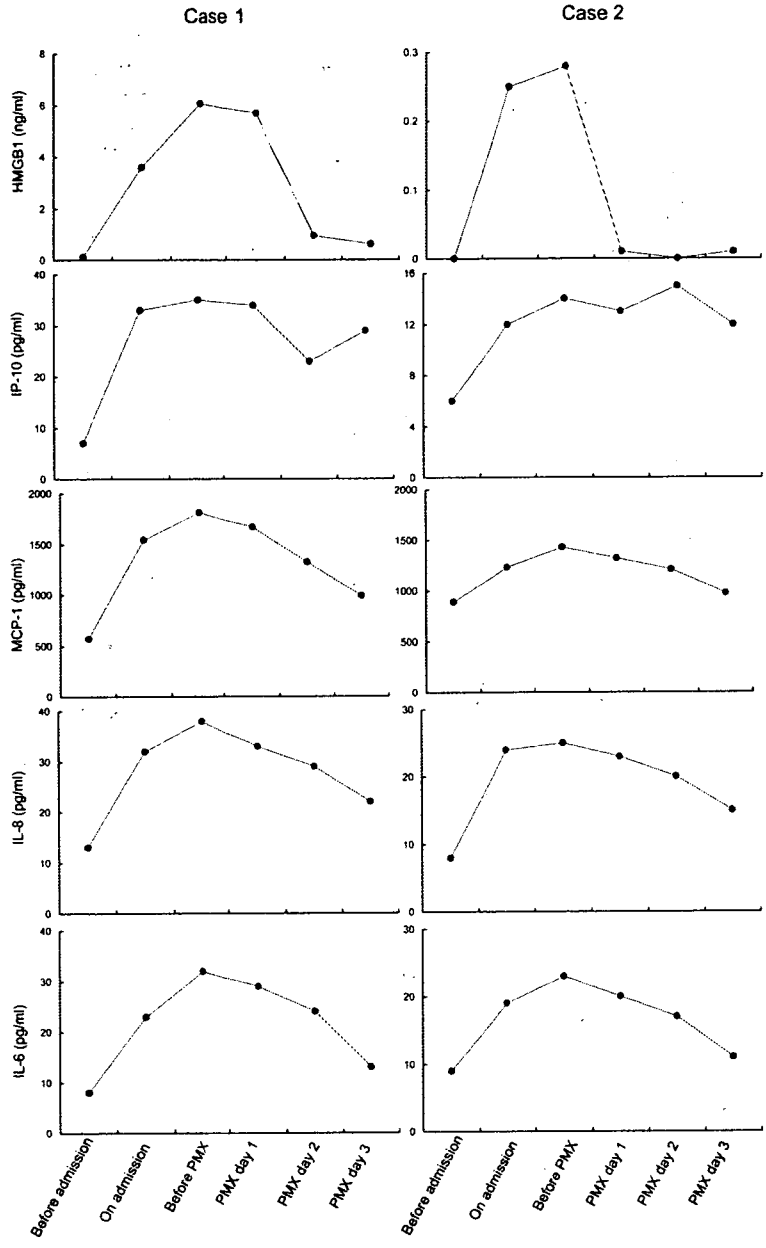

Figure 3. Cytokine changes in sera of our cases during the PMX hemoperfusion treatment. The serum HMGB1 level was undetectable before admission, increased on admission, and decreased remarkably on day 2 after the start of PMX hemoperfusion treatment in both cases. The serum level of IP-10 did not show remarkable change during the PMX hemoperfusion treatment. The serum level of MCP-1, IL-8, and IL-6 decreased on day 3 after the start of PMX hemoperfusion treatment, but was higher than before admission in both cases.

ter admission.

Criteria for the PMX hemoperfusion treatment on acute exacerbation of interstitial pneumonia

As a policy of our department, we administrate PMX hemoperfusion to the patients who fulfill the following criteria: 1) acute exacerbation of interstitial pneumonia; 2) no obvious evidence of infectious disease; 3) P/F ratio does not increase above 300 (criteria for acute lung injury (13)) within 24 hours despite the start of standard treatments for acute exacerbation of interstitial pneumonia.

Measurement of serum cytokine level

We measured interleukin-6 (IL-6), IL-8, monocyte chemoattractant protein-1 (MCP-1) and interferon inducible protein of 10 kDa (IP-10) levels in sera of our patients using a commercial enzyme-linked immunosorbent assay (ELISA) kit (sIL-2R: R&D Systems, Minneapolis, MN). ELISA for high mobility group box 1 (HMGB1) in the sera was performed with the use of monoclonal antibodies to HMGB1 and with standardization to a curve of recombinant human HMGB1 as described previously (14). As shown in Fig. 3, The serum HMGB1 level was undetectable before admission, increased on admission, and decreased remarkably on day 2 after the

start of PMX hemoperfusion treatment in both cases. The serum level of IP-10 did not show a remarkable change during the PMX hemoperfusion treatment. The serum levels of MCP-1, IL-8, and IL-6 decreased on day 3 after the start of PMX hemoperfusion treatment, but were higher than before admission in both cases.

Flow cytometry analysis of BALF cells

The expression of BALF cell surface CD3, CD18, CD11c, CD25 (interleukin-2 receptor), CXCR2 (receptor of IL-8), CXCR3 (receptor for IP-10) and CCR2 (receptor of MCP-1) (15) was evaluated by flow-cytometry analysis. One hundred thousand BALF cells were suspended in 50 μl of cold PBS containing 0.1% sodium azide, 10 ng/ml BSA and 20 μg/ml of human IgG, incubated for 10 minutes on ice, and with mouse monoclonal anti-CXCR2, CD18, CCR2, CXCR3 or CD25 (PharMingen, SanDiego, CA, USA) IgG antibody and FITC-conjugated anti-CD3 or PE-conjugated CD11c antibody (PharMingen) for an additional 15 minutes on ice. Cells were washed with PBS, and incubated with FITC or PE-conjugated goat anti-mouse IgG for 15 minutes on ice. At the end of the incubation, 7AAD (PharMingen) was added to each tube. The cells were washed with PBS, and subsequently analyzed by flow cytometry using a FACScan (Becton Dickinson). Dead cells, determined by the incorporation of 7AAD, were gated out. Results were processed using the CellQuest software (Becton Dickson).

As shown in Table 1, the percentage of CD18+/CD11c+, CCR2+, and/CXCR2+BALF cell decreased remarkably while CD3+/CD25+ and CXCR3+ BALF cell percentage did not show remarkable change.

Discussion

Acute exacerbations of IPs have been described to have high mortality during short course (3, 6, 7). Recent reports have suggested that PMX hemoperfusion treatment may be effective in patients with ALI/ARDS and acute exacerbation of IPF (8, 9, 11). PMX hemoperfusion treatment can reduce the mortality of ARDS (11) and reduce serum level of metalloproteinase (MMP)-9 tissue inhibitor of MMP (TIMP)-1 (9). Also, PMX hemoperfusion treatment can improve the survival rate of sepsis with renal failure (16) and oxygenation of sepsis patients (17). In particular, Seo et al reported that four of six patients of acute exacerbations of IPF were successfully weaned from mechanical ventilation and survived more than 30 days after the initial PMX hemoperfusion treatment, suggesting the clinical effect of PMX hemoperfusion treatment (10). The present cases also survived more than 30 days, however, the outcome of our two cases was totally different (case 1 died while case 2 is still alive on April 25, 2007). We think this difference might have been due to the following reasons: 1) The difference of timing of PMX hemoperfusion administration [Early administration of PMX hemoperfusion treatment can eliminate humoral mediators and improves pulmonary oxygenation.]. (8); 2) The presence of infection in case 1 (Case 1 showed bronchopneumonia at autopsy). However, it is difficult to determine the true reason for this difference. Detection of the true reason of this difference might provide an important insight to clarify the mechanism of PMX treatment in acute exacerbation of interstitial pneumonia.

The detailed mechanism by which PMX hemoperfusion treatment improves oxygenation has not been fully elucidated. In the present cases, we showed a decrease of IL-8, MCP-1, IL-6, and HMGB1 level in the sera, however, the serum IP-10 level did not change remarkably during the PMX treatment. IL-8, a chemokine that can activate neutrophils through CXCR2 (15), is elevated in IPF and indicates disease activity (18) and is associated with the pathogenesis of MPO-ANCA vasculitis (19). MCP-1, a chemokine that can attract a variety of inflammatory cells including monocytes and neutrophils (15), is a marker of ANCA-associated vasculitis (20) and is involved in the pathogenesis of IPF (21). PMX hemoperfusion treatment can reduce the serum level of IL-6 and HMGB1 (22). IL-6 is an important inflammatory mediator (23). HMGB-1 has recently been proposed as one of the late mediators of sepsis or lipopolysaccharide (LPS) endotoxin lethality (24). Abraham et al demonstrated that the intratracheal administration of recombinant HMGB-1 is a distal mediator of acute inflammatory lung injury (25). Ueno et al suggested that the overexpression of extracellular HMGB-1 plays a key role in the pathogenesis of ALI (26). The modification of these cytokines might be associated with the effect of PMX hemoperfusion treatment on acute exacerbation of interstitial pneumonia.

In the present cases, CD18+/CD11c+ and CXCR2+ BALF cell percentage decreased after the PMX hemoperfusion treatment. CD18+/CD11c+ is a marker of activated neutrophils (27), and CXCR2 is a receptor of IL-8 (15). In our report, we found that a decrease in cytokine is associated with activation of neutrophils. This change might contribute to the decrease of CD18+CD11c positive cells. However, the reason for the increase in neutrophil % after the PMX treatment in case 2 is still unclear. Ambrosini et al reported that in acute exacerbations of IPF, marked neutrophilia was detected in BALF (3). Neutrophils cause damage to the pulmonary vascular endothelium by releasing oxygen radicals, proteinases, leukotrienes, and other proinflammatory molecules such as platelet-activating factor, thus impairing the barrier function of the pulmonary capillaries and leading to the onset of ALI or ARDS (28, 29). In our cases, CCR2+ BALF cell percentage decreased after the PMX hemoperfusion treatment. MCP-1-CCR2 axis contributes to the neutrophil recruitment in lung via alveolar macrophages in lung inflammation (30). In the present cases, CD3+/CD25+ BALF cell percentage and CXCR3 (receptor for of IP-10 (15)) positive cell percentage did not show remarkable change. CD3+/CD25+ cells are activated T lymphocytes (31), and IP-10 is a chemokine that can recruit activated T lymphocytes (32). These results may suggest the relation between the effect of PMX hemoperfusion treatment and acti-

DOI: 10.2169/internalmedicine.46.0117

vated neutrophils. In summary, we reported two cases of acute exacerbation of interstitial pneumonia who received polymyxin B-immobilized fiber column hemoperfusion treatment. Also, our report showed flow-cytometry analysis of BALF cells and a change in the serum HMGB1 level that was not investigated in previous reports. Further accumulation of clinical data concerning this point might bring new insight to clarify the detailed mechanism by which PMX hemoperfusion treatment improves oxygenation.

We wish special thanks to Mrs. Rumi Matsuyama (Third Department of Internal Medicine, Kagoshima University Faculty of Medicine) for her excellent help.

References

1. Kondoh Y, Taniguchi H, Kawabata Y, Yokoi T, Suzuki K, Takagi K. Acute exacerbation in idiopathic pulmonary fibrosis. Analysis of clinical and pathologic findings in three cases. Chest **103**: 1808-1812, 1993.
2. Parambil JG, Myers JL, Ryu JH. Histopathologic features and outcome of patients with acute exacerbation of idiopathic pulmonary fibrosis undergoing surgical lung biopsy. Chest **128**: 3310-3315, 2005.
3. Ambrosini V, Cancellieri A, Chilosi M, et al. Acute exacerbation of idiopathic pulmonary fibrosis: report of a series. Eur Respir J **22**: 821-826, 2003.
4. Parambil JG, Myers JL, Ryu JH. Diffuse alveolar damage: uncommon manifestation of pulmonary involvement in patients with connective tissue diseases. Chest **130**: 553-558, 2006.
5. Parambil JG, Myers JL, Lindell RM, Matteson EL, Ryu JH. Interstitial lung disease in primary Sjögren syndrome. Chest **130**: 1489-1495, 2006.
6. Akira M, Hamada H, Sakatani M, Kobayashi C, Nishioka M, Yamamoto S. CT findings during phase of accelerated deterioration in patients with idiopathic pulmonary fibrosis. AJR Am J Roentgenol **168**: 79-83, 1997.
7. Rice AJ, Wells AU, Bouros D, et al. Terminal diffuse alveolar damage in relation to interstitial pneumonias. An autopsy study. Am J Clin Pathol **119**: 709-714, 2003.
8. Kushi H, Miki T, Okamaoto K, Nakahara J, Saito T, Tanjoh K. Early hemoperfusion with an immobilized polymyxin B fiber column eliminates humoral mediators and improves pulmonary oxygenation. Crit Care **9**: R653-R661, 2005.
9. Nakamura T, Kawagoe Y, Matsuda T, et al. Effect of polymyxin B-immobilized fiber on blood metalloproteinase-9 and tissue inhibitor of metalloproteinase-1 levels in acute respiratory distress syndrome patients. Blood Purif **22**: 256-260, 2004.
10. Seo Y, Abe S, Kurahara M, et al. Beneficial effect of polymyxin B-immobilized fiber column (PMX) hemoperfusion treatment on acute exacerbation of idiopathic pulmonary fibrosis. Intern Med **45**: 1033-1038, 2006.
11. Tsushima K, Kubo K, Koizumi T, et al. Direct hemoperfusion using a polymyxin B immobilized column improves acute respiratory distress syndrome. J Clin Apher **17**: 97-102, 2002.
12. American Thoracic Society/European Respiratory Society International Multidisciplinary Consensus Classification of the Idiopathic Interstitial Pneumonias. This joint statement of the American Thoracic Society (ATS), and the European Respiratory Society (ERS) was adopted by the ATS board of directors, June 2001 and by the ERS Executive Committee, June 2001. Am J Respir Crit Care Med **165**: 277-304, 2002.
13. Bernard GR, Artigas A, Brigham KL, et al. The American-European Consensus Conference on ARDS. Definitions, mechanisms, relevant outcomes, and clinical trial coordination. Am J Respir Crit Care Med **149**: 818-824, 1994.
14. Yamada S, Inoue K, Yakabe K, Imaizumi H, Maruyama I. High mobility group protein 1 (HMGB1) quantified by ELISA with a monoclonal antibody that does not cross-react with HMGB2. Clin Chem **49**: 1535-1537, 2003.
15. Rollins BJ. Chemokines. Blood **90**: 909-928, 1997.
16. Suzuki H, Nemoto H, Nakamoto H, et al. Continuous hemodiafiltration with polymyxin-B immobilized fiber is effective in patients with sepsis syndrome and acute renal failure. Ther Apher **6**: 234-240, 2002.
17. Naka T, Shinozaki M, Akizawa T, Shima Y, Takaesu H, Nasu H. The effect of continuous veno-venous hemofiltration or direct hemoperfusion with polymyxin B-immobilized fiber on neutrophil respiratory oxidative burst in patients with sepsis and septic shock. Ther Apher Dial **10**: 7-11, 2006.
18. Ziegenhagen MW, Zabel P, Zissel G, Schlaak M, Muller-Quernheim J. Serum level of interleukin 8 is elevated in idiopathic pulmonary fibrosis and indicates disease activity. Am J Respir Crit Care Med **157**: 762-768, 1998.
19. Hsieh SC, Yu HS, Cheng SH, et al. Anti-myeloperoxidase antibodies enhance phagocytosis, IL-8 production, and glucose uptake of polymorphonuclear neutrophils rather than anti-proteinase 3 antibodies leading to activation-induced cell death of the neutrophils. Clin Rheumatol **26**: 216-224, 2007.
20. Tam FW, Sanders JS, George A, et al. Urinary monocyte chemoattractant protein-1 (MCP-1) is a marker of active renal vasculitis. Nephrol Dial Transplant **19**: 2761-2768, 2004.
21. Matsuyama W, Watanabe M, Shirahama Y, et al. Activation of discoidin domain receptor 1 on CD14-positive bronchoalveolar lavage fluid cells induces chemokine production in idiopathic pulmonary fibrosis. J Immunol **174**: 6490-6498, 2005.
22. Sakamoto Y, Mashiko K, Matsumoto H, et al. Effect of direct hemoperfusion with a polymyxin B immobilized fiber column on high mobility group box-1 (HMGB-1) in severe septic shock: report of a case. ASAIO J **52**: e37-e39, 2006.
23. Gabay C. Interleukin-6 and chronic inflammation. Arthritis Res Ther **8** (Suppl 2): S3, 2006.
24. Wang H, Bloom O, Zhang M, et al. HMG-1 as a late mediator of endotoxin lethality in mice. Science **285**: 248-251, 1999.
25. Abraham E, Arcaroli J, Carmody A, Wang H, Tracey KJ. HMG-1 as a mediator of acute lung inflammation. J Immunol **165**: 2950-2954, 2000.
26. Ueno H, Matsuda T, Hashimoto S, et al. Contributions of high mobility group box protein in experimental and clinical acute lung injury. Am J Respir Crit Care Med **170**: 1310-1316, 2004.
27. Berton G, Laudanna C, Sorio C, Rossi F. Generation of signals activating neutrophil functions by leukocyte integrins: LFA-1 and gp150/95, but not CR3, are able to stimulate the respiratory burst of human neutrophils. J Cell Biol **116**: 1007-1017, 1992.
28. Ware LB, Matthay MA. The acute respiratory distress syndrome. N Engl J Med **342**: 1334-1349, 2000.
29. Dudek SM, Garcia JG. Cytoskeletal regulation of pulmonary vascular permeability. J Appl Physiol **91**: 1487-1500, 2001.
30. Maus UA, Waelsch K, Kuziel WA, et al. Monocytes are potent facilitators of alveolar neutrophil emigration during lung inflammation: role of the CCL2-CCR2 axis. J Immunol **170**: 3273-3278, 2003.
31. Smith KA. The interleukin 2 receptor. Annu Rev Cell Biol **5**: 397-425, 1989.

DOI: 10.2169/internalmedicine.46.0117

32. Loetscher M, Gerber B, Loetscher P, et al. Chemokine receptor specific for IP10 and mig: structure, function, and expression in activated T-lymphocytes. J Exp Med **184**: 963-969, 1996.

MOLECULAR AND CELLULAR BIOLOGY, Aug. 2007, p. 5650–5663 Vol. 27, No. 16
0270-7306/07/$08.00+0 doi:10.1128/MCB.00130-07

Stage-Specific Secretion of HMGB1 in Cartilage Regulates Endochondral Ossification▽†

Noboru Taniguchi,[1] Kenji Yoshida,[1] Tatsuo Ito,[1] Masanao Tsuda,[1] Yasunori Mishima,[1] Takayuki Furumatsu,[1] Lorenza Ronfani,[2] Kazuhiro Abeyama,[4] Ko-ichi Kawahara,[4] Setsuro Komiya,[5] Ikuro Maruyama,[4] Martin Lotz,[1] Marco E. Bianchi,[2,3] and Hiroshi Asahara[1,6,7]*

Department of Molecular and Experimental Medicine, The Scripps Research Institute, 10550 North Torrey Pines Road, La Jolla, California 92037[1]; DIBIT, San Raffaele Scientific Institute, via Olgettina 58, 20132 Milano, Italy[2]; San Raffaele University, via Olgettina 58, 20132 Milano, Italy[3]; Department of Laboratory and Vascular Medicine, Graduate School of Medical and Dental Sciences, Kagoshima University, 8-35-1 Sakuragaoka, Kagoshima 890-8520, Japan[4]; Department of Orthopaedic Surgery, Graduate School of Medical and Dental Sciences, Kagoshima University, 8-35-1 Sakuragaoka, Kagoshima 890-8520, Japan[5]; National Center for Child Health and Development, 2-10-1 Okura, Setagaya, Tokyo 157-8535, Japan[6]; and SORST, Japan Science and Technology Agency, 4-1-8 Honcho, Kawaguchi, Saitama 332-0012, Japan[7]

Received 20 January 2007/Returned for modification 25 February 2007/Accepted 19 May 2007

High mobility group box 1 protein (HMGB1) is a chromatin protein that has a dual function as a nuclear factor and as an extracellular factor. Extracellular HMGB1 released by damaged cells acts as a chemoattractant, as well as a proinflammatory cytokine, suggesting that HMGB1 is tightly connected to the process of tissue organization. However, the role of HMGB1 in bone and cartilage that undergo remodeling during embryogenesis, tissue repair, and disease is largely unknown. We show here that the stage-specific secretion of HMGB1 in cartilage regulates endochondral ossification. We analyzed the skeletal development of *Hmgb1*$^{-/-}$ mice during embryogenesis and found that endochondral ossification is significantly impaired due to the delay of cartilage invasion by osteoclasts, osteoblasts, and blood vessels. Immunohistochemical analysis revealed that HMGB1 protein accumulated in the cytosol of hypertrophic chondrocytes at growth plates, and its extracellular release from the chondrocytes was verified by organ culture. Furthermore, we demonstrated that the chondrocyte-secreted HMGB1 functions as a chemoattractant for osteoclasts and osteoblasts, as well as for endothelial cells, further supporting the conclusion that *Hmgb1*$^{-/-}$ mice are defective in cell invasion. Collectively, these findings suggest that HMGB1 released from differentiating chondrocytes acts, at least in part, as a regulator of endochondral ossification during osteogenesis.

Bone formation occurs through two developmental processes: intramembranous ossification and endochondral ossification. Intramembranous ossification takes place in several craniofacial bones and the lateral part of clavicles, whereas endochondral ossification occurs in the long bones of the limbs, the basal part of the skull, vertebrae, ribs, and the medial part of the clavicles. In endochondral ossification, an intermediate step occurs during which cartilaginous templates prefigure future skeletal elements and play a major role in regulating the developing skeletal elements (33). First, mononucleated osteoclast precursors enter the mesenchyme surrounding the bone rudiments, proliferate, differentiate into tartrate-resistant acid phosphatase (TRAP)-positive cells, and migrate together with endothelial cells through the nascent bone collar (7). Subsequently, they invade the calcified cartilage, filling the core of the diaphysis while fusing and differentiating into mature osteoclasts, and transform the core of the bone into a marrow cavity (15). Osteoclasts are derived from hematopoietic precursor cells formed by the fusion of monocytic cells at the bone sites to be resorbed, whereas osteoblasts arise from multipotential mesenchymal cells and further differentiate into bone-lining cells and osteocytes (30).

These events, including osteoclast migration and angiogenesis during endochondral ossification, are tightly coordinated by extracellular factors, such as matrix metalloproteinases (MMPs) and vascular endothelial growth factor (VEGF) (37). When neovascularization of the cartilage anlage begins, membrane type 1 MMP (MT1-MMP) and MMP9 are expressed in the preosteoclasts and other chondroclastic cells of unknown origins (23). Mice deficient in *Mmp9* exhibit a delay in osteoclast recruitment in specialized invasion and bone resorption models in vitro (15). It is also reported that the deletion of functional *Mmp13* has profound effects on skeletal development (25). In *Mmp13*-null embryos, the growth plates were strikingly lengthened, a defect related predominantly to a delay in terminal events in the growth plates, with failure to resorb collagens, as well as a delay in ossification at the primary centers. In addition, VEGF signaling plays an important role of angiogenesis during skeletal development (59). Inhibition of VEGF by the administration of a soluble chimeric VEGF receptor protein to 24-day-old mice inhibited blood vessel invasion

* Corresponding author. Mailing address: Department of Molecular and Experimental Medicine, The Scripps Research Institute, 10550 North Torrey Pines Road, La Jolla, CA 92037. Phone: (858) 784-9026. Fax: (858) 784-2744. E-mail: asahara@scripps.edu.

† Supplemental material for this article may be found at http://mcb.asm.org/.

▽ Published ahead of print on 4 June 2007.

into the hypertrophic zone of long bone growth plates and resulted in impaired trabecular bone formation and expansion of the hypertrophic zone (17).

High mobility group box 1 protein (HMGB1) is a chromatin protein that is widely expressed and extremely conserved in mammals. There are three HMGB proteins: HMGB1, HMGB2, and HMGB3 with >80% amino acid identity, which are composed of two basic HMG-box domains (A and B) and a long acidic C-terminal tail (10). As a nuclear factor, HMGB1 acts as an architectural protein that can bend DNA to promote nucleoprotein interactions and facilitate diverse DNA modifications (2). Several groups have shown that HMGB1 also has an extracellular role as a proinflammatory cytokine (4, 51, 55). Two different routes for HMGB1 release into the extracellular milieu have been reported: active secretion by activated macrophages and monocytes (54) and passive release from necrotic or damaged cells (45). HMGB1 released by damaged cells acts as a chemoattractant for vascular smooth muscle cells and fibroblasts and induces cytoskeleton reorganization and cell migration (13). HMGB1 also promotes the migration of local stem cells, such as vessel-associated stem cells (mesoangioblasts) (38), and endothelial cells (32, 46), suggesting that HMGB1 is tightly connected to the process of tissue organization. The biological relevance of HMGB1 in vivo was shown in *Hmgb1*$^{-/-}$ mice, which have a highly pleiotropic phenotype such as the inability to use glycogen stored in the liver (11). These mice survive for several days if given glucose parenterally; however, mutants remained much smaller than control littermates and had arched backs, posterior limbs splayed wide apart, and abnormal gait. These findings suggested that HMGB1 may participate in not only tissue repair after injury but also the organization of bone and cartilage development.

We show here that the stage-specific secretion of HMGB1 in cartilage regulates endochondral ossification, in part, by acting as a chemotactic factor for the cells that invade at the primary ossification center. These findings highlight the potential role of HMGB1 in skeletal homeostasis.

MATERIALS AND METHODS

Mice. The *Hmgb1*$^{-/-}$ mutant mice used in the present study were described before (11), except for their background, which is now pure BALB/c. All animal experiments were performed according to approved protocols according to institutional guidelines at The Scripps Research Institute. Mouse embryos for histomorphometry were littermates from *Hmgb1*$^{+/-}$ parents. The genotype of the mice was determined by PCR analysis of tail DNA. The wild-type *Hmgb1* allele was detected by PCR with the primers wildtype-1 (5′-GCA GGC TTC GTT GTT TTC ATA CAG-3′) and wildtype-2 (5′-TCA AAG AGT AAT ACT GCC ACC TTC-3′), which generate a 495-bp fragment. The mutant *Hmgb1* allele was detected by using two primers complementary to the neomycin resistance gene—Neo-1 (5′-TGG TTT GCA GTG TTC TGC CTA GC-3′) and Neo-2 (5′-CCC AGT CAT AGC CGA ATA GCC-3′)—which generate a 336-bp fragment.

Histological analysis. Mice were sacrificed at various embryonic stages, dissected, and fixed in 4% paraformaldehyde–phosphate-buffered saline at 4°C overnight. Subsequently, they were processed, embedded in paraffin, and sectioned. For HMGB1 immunostaining, rabbit anti-HMGB1 antibody (Pharmingen, San Diego, CA) and chicken anti-HMGB1 antibody (Shino-Test, Kanagawa, Japan) were used for limb sections and organ culture sections, respectively (51). For CD31 immunostaining, embryos were infiltrated in 20% sucrose, followed by OCT embedding to stain with rat anti-PECAM antibody (Pharmingen) and von Kossa and Safranin O/Fast Green staining (47). Whole-mount alcian blue and alizarin red S staining of skeletons were done as described previously (31), and the longitudinal diameters of calvariae, as well as the lengths and alizarin-positive regions of tibias, were measured by micrometer. Detection of apoptotic cells in paraffin sections of limbs was based on a modification of genomic DNA utilizing terminal deoxynucleotidyl transferase (TUNEL [terminal deoxynucleotidyltransferase-mediated dUTP-biotin nick end labeling] assay) and indirect detection of positive cells by fluorescein conjugated anti-digoxigenin antibody using a MEBSTAIN Apoptosis Kit Direct (Medical and Biological laboratories, Nagoya, Japan). Immunofluorescence assay to determine HMGB1 translocation in chondrocytes was carried out with rabbit anti-HMGB1 antibody (Pharmingen) as described before (51).

Using a leukocyte acid phosphatase kit from Sigma (St. Louis, MO), TRAP staining was performed on paraffin sections according to the instructions provided by the manufacturer. The determination of the numbers and distribution of TRAP-positive cells in longitudinal sections of bones was done as described previously (7, 56).

In situ hybridization. Tissues were fixed in 4% paraformaldehyde–phosphate-buffered saline overnight at 4°C, processed, embedded in paraffin, and sectioned. RNA in situ hybridization was performed as described previously (3). Briefly, slides were deparaffinized, treated with proteinase K (1 μg/ml) for 20 min at 37°C, and hybridized with ^{35}S-labeled antisense riboprobes in hybridization buffer (50% deionized formamide, 300 mM NaCl, 20 mM Tris-HCl [pH 8.0], 5 mM EDTA, 0.5 mg of yeast tRNA/ml, 10% dextran sulfate, and 1× Denhardt solution) in a humidified chamber at 60°C overnight. After hybridization, the slides were treated with RNase A, washed to a final stringency of 50% formamide, 2× SSC (1× SSC is 0.15 M NaCl plus 0.015 M sodium citrate) at 60°C, dipped in emulsion, exposed for 3 days to 3 weeks, and developed. The probes for Indian hedgehog, MMP9, VEGF and MMP13, MT1-MMP, Runx2 and Osterix, and osteocalcin and osteopontin were provided by Y. Kawakami (Salk Institute), S. M. Krane (Harvard Medical School), Z. Werb (University of California, San Francisco), T. Vu (University of California, San Francisco), K. Nakashima (Tokyo Medical and Dental University), and S. Nomura (Osaka University Graduate School of Medicine), respectively. The HMGB1 probe was a 1.2-kb cDNA fragment encoding the COOH-terminal domain and the 3′-untranslated region (UTR). The Col1a1 probe was a 0.8-kb cDNA fragment encoding the COOH-terminal domain.

Organ culture. Metatarsal bones and tibiae were harvested from mouse embryos at embryonic day 15.5 (E15.5) and E14.5, respectively. They were cultured for 5 days in conditioned medium as described previously (20). The expression levels of HMGB1 and lactate dehydrogenase (LDH) in the supernatant were assessed by immunoblotting with rabbit anti-HMGB1 antibody (Pharmingen) and goat anti-LDH antibody (Chemicon, Temecula, CA) as described previously (45). Rib chondrocytes were purified from the ventral parts of rib cartilage of 2- to 4-day-old BALB/c mice (28), followed by induction of necrosis as described previously (45), and were used as a positive control for the HMGB1 protein. The concentrations of HMGB1 released into conditioned supernatant were measured in triplicate with an enzyme-linked immunosorbent assay (ELISA) using commercially available kits (Shino-Test) (57).

Preparation of osteoclasts and osteoblasts. Human osteoclast precursor cells (Poietics; Cambrex Bio Science Walkersville, Inc., Walkersville, MD) were cultured in alpha-minimal essential medium (alpha-MEM) containing 10% fetal bovine serum, penicillin-streptomycin, and HEPES containing alpha-MEM medium with receptor activator of nuclear factor B ligand (RANKL; PeproTech EC, Ltd., London, United Kingdom) and M-CSF (R&D Systems, Minneapolis, MN). Cells were incubated in a CO_2 incubator in a humidified atmosphere of 95% air and 5% CO_2 at 37°C. After complete osteoclast differentiation at day 7, the medium was replaced with serum-free alpha-MEM; the cells were starved for 2 h and then used for chemotaxis assays. MC3T3-E1 osteoblastic cells were purchased from the American Type Culture Collection (Manassas, VA) and cultured in alpha-MEM with 10% fetal bovine serum.

Chemotaxis assays. Chemotaxis assays were performed as described previously (22). The assays were carried out in Boyden chambers with polycarbonate filters with 9-μm pores (Corning Costar, Corning, NY). Osteoclasts were prepared by sequential treatment with trypsin, and the remaining cells were then gently lifted off the plates with a rubber policeman. The osteoclasts were seeded in 48-transwell plates in alpha-MEM containing 0.1% (wt/vol) Albumax and kept for 4 h with or without addition of rat cytokine-quality HMGB1 (obtained from HMGBiotech, Milan, Italy) and VEGF (R&D Systems). Invasion was determined as the ratio of osteoclasts that migrated through the collagen gel to reach the lower side of the membrane compared to the total number of osteoclasts in the insert. The chemotaxis assays for MC3T3-E1 cells were also performed

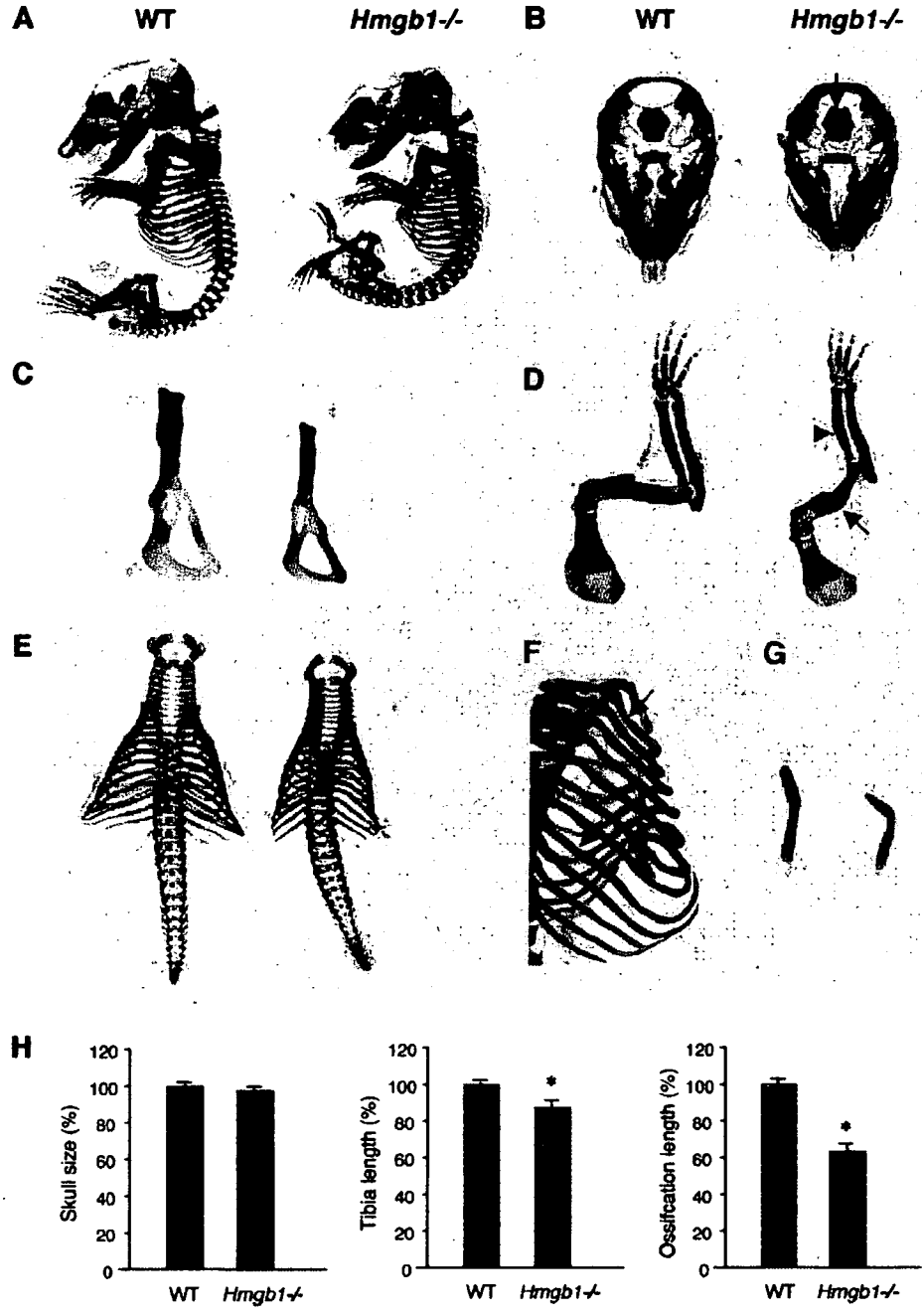

FIG. 1. Analysis of skeletal development in *Hmgb1*$^{-/-}$ mice by double staining with alcian blue and alizarin red. (A) *Hmgb1*$^{-/-}$ embryos (right) are smaller than wild-type (WT) littermates (left) at E16.5. (B) At this stage, facial and skull bones formed by intramembranous ossification appear similar between two groups, whereas sphenoid bones (arrowhead) and basioccipital (arrow) of the chondrocranium, which are formed by endochondral ossification, appear reduced in size and in intensity of alizarin red staining in *Hmgb1*$^{-/-}$ embryos. (C) The pelvis has smaller alizarin red-stained zones in *Hmgb1*$^{-/-}$ embryos. (D) The radius and ulna in *Hmgb1*$^{-/-}$ forelimbs are not only reduced in size and calcification, but bent (arrowhead); the humerus is often fractured (arrow). The thorax in *Hmgb1*$^{-/-}$ embryos shows severe hypoplasia accompanied by spinal scoliosis (E) and kyphosis (A). Ribs stained less intensely for alizarin red and are thin and bent (arrows) (F), and clavicles are hypoplastic and crooked in *Hmgb1*$^{-/-}$ embryos (G). (H) Statistical comparison between wild-type (n = 6) and *Hmgb1*$^{-/-}$ (n = 6) embryos at E16.5. The wild type is defined as 100%. Diameters of calvariae (skull size): wild-type, 100% ± 2.7%; mutant, 97.7% ± 2.2% (no statistical difference). Tibia length: wild-type, 100% ± 1.6%; mutant, 87.4% ± 6.9% ($P < 0.001$). Length of the ossified zone (alizarin red positive) of tibia: wild-type, 100% ± 6.9%; mutant, 63.6% ± 9.6% ($P < 0.0001$). The asterisk indicates a significant statistical difference ($P < 0.01$).

according to the method as described above. All experiments were performed at least twice in four replicates.

Three-dimensional pellet culture. Mice rib chondrocytes were prepared from the ventral parts rib cartilage of 2- to 4-day-old C57BL/6 mice as described previously (36). Human articular chondrocytes were isolated from human cartilage, and a primary cell culture was established (21). Both types of chondrocytes were cultured in three-dimensional cell pellets for 18 days as described before (5). Briefly, 1-ml aliquots containing 2 × 10^5 cells each were added to 15-ml

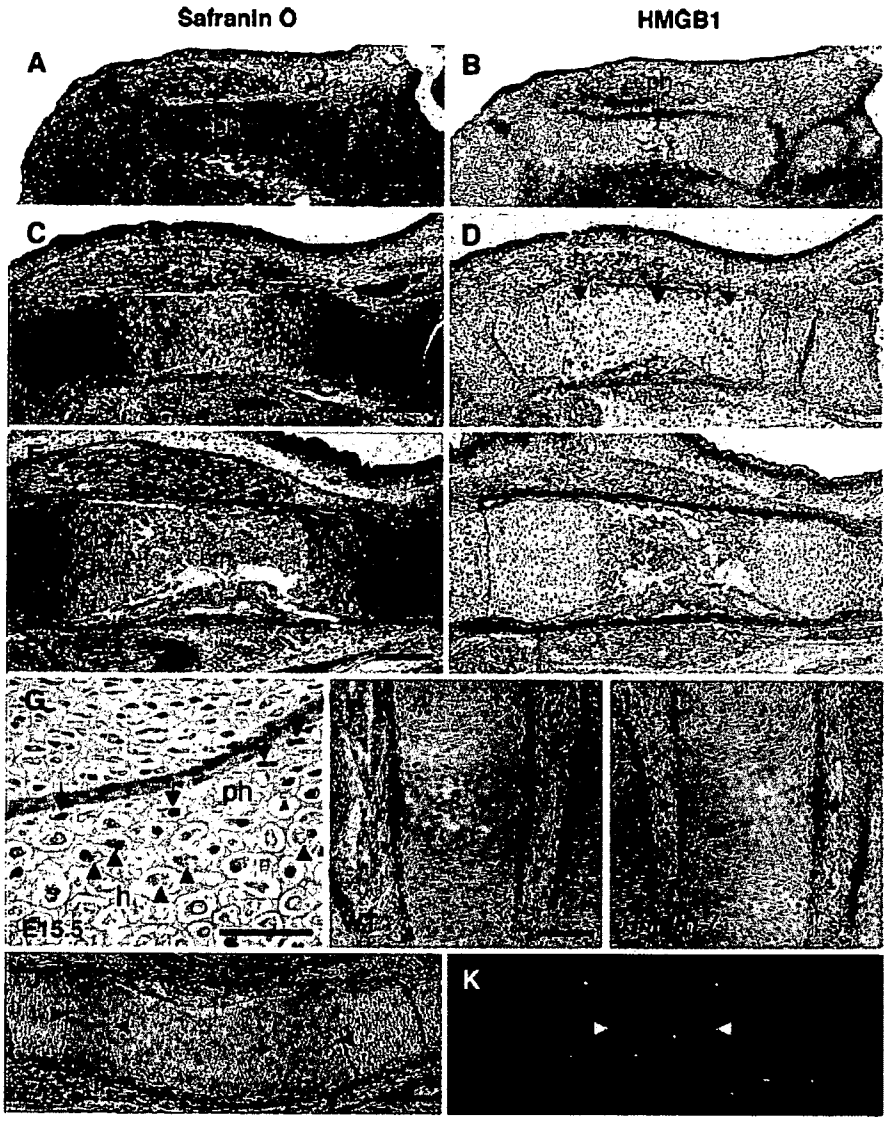

FIG. 2. Localization of HMGB1 protein in developing limbs. Adjacent sections of tibia were stained with safranin O (A, C, and E) and antibody to HMGB1 (B, D, and F). HMGB1 is expressed in the prehypertrophic chondrocytes at E14.5 (B) and in the hypertrophic chondrocytes at E15.5 (D). In contrast, resting and proliferating chondrocytes do not show any positive staining in either nuclei or cytoplasm. (F) Expression is robust in the limbs at E14.5 and E15.5 but attenuates at E16.5. (G) Large magnifications of the humerus at E15.5. HMGB1 is positive in the nuclei of prehypertrophic chondrocytes (arrows) and in the cytosol of hypertrophic chondrocytes (arrowheads). (H) At E16.5, metacarpal bones also show HMGB1 expression in the nuclei of prehypertrophic chondrocytes, as well as in the cytoplasm of hypertrophic chondrocytes. (I) The positive staining in hypertrophic cartilage is absent in sections from *Hmgb1*$^{-/-}$ metacarpal bones at E16.5. The staining in perichondrium is nonspecific (arrowheads). (J and K) Analysis of HMGB1 expression and apoptosis in radius at E15.5. Arrowheads indicate the HMGB1-positive cells (J) and TUNEL-positive cells presenting apoptosis of hypertrophic chondrocytes (K). ph, prehypertrophic cartilage; h, hypertrophic cartilage; c, calcified cartilage; bm, bone marrow. Scale bars: A to F, J, and K, 200 μm; G to I, 50 μm.

conical polypropylene centrifuge tubes (Becton Dickinson, San Diego, CA), and the cells were pelleted by centrifugation at 600 rpm for 5 min at room temperature. The cultures were maintained at 37°C in 5% CO_2 in a humidified incubator. Pellets were maintained up to 18 days in Dulbecco modified Eagle medium–F-12 supplemented with 50 μg of ascorbate phosphate (Sigma)/ml, 100 μg of pyruvate/ml, 1% penicillin-streptomycin (Gibco, Grand Island, NY), and 50 mg of ITS+Premix (Becton Dickinson, Bedford, MA; a final concentration of 6.25 μg of bovine insulin/ml, 6.25 μg of transferrin/ml, 6.25 ng of selenous acid/ml, 1.25 mg of bovine serum albumin/ml, and 5.35 μg of linoleic acid/ml)/ml. The medium was changed every 3 days. Cryostat-sectioned pellets were used for immunofluorescence assay. The supernatant of pelleted mouse rib chondrocytes and human articular chondrocytes was used for chemotaxis assay with or without addition of anti-HMGB1 IgY neutralizing HMGB1, a gift from Shino-Test (1), and control IgY (Promega, Madison, WI).

Quantitative PCR. Total RNA was extracted and oligo(dT)-primed cDNA was prepared from 500 ng of total RNA by using Superscript II (Invitrogen, Carlsbad, CA). The resulting cDNAs were analyzed by using the SYBR green system for quantitative analysis of specific transcripts according to the manufacturer's instructions (Applied Biosystems, Foster City, CA). All mRNA expression data were normalized to GAPDH expression in the corresponding sample. The primers used in real-time PCR are as follows: Col10a1, 5′-GCCTCAAATACCCTT TCTGC (sense) and 5′-GTGTCTTGGGGCTAGCAAGT (antisense); MMP13, 5′-GAAGACCTTGTGTTTGCAGAGC (sense) and 5′-CTCGGAGCCTGTCA ACTGTG (antisense); Hmgb1, 5′-GGCTGACAAGGCTCGTTATG (sense)

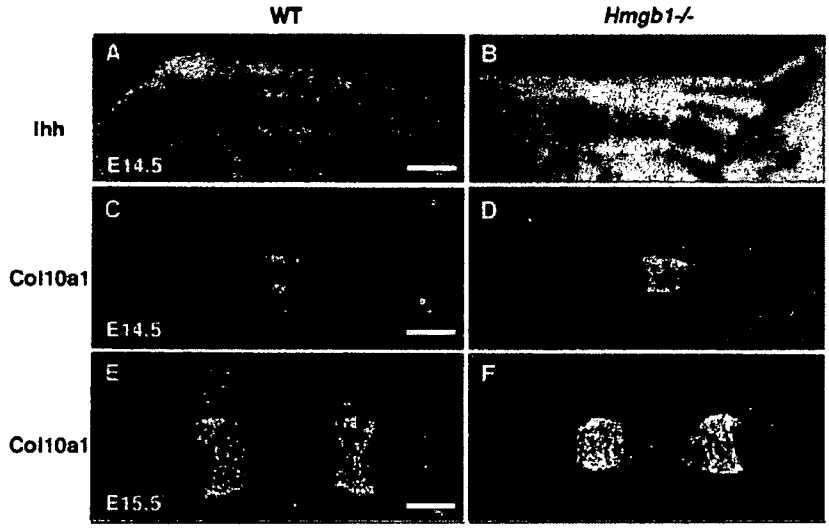

FIG. 3. Expression of chondrocyte differentiation markers in wild-type and *Hmgb1*$^{-/-}$ tibia. (A and B) Indian hedgehog (Ihh) is comparable between wild-type and *Hmgb1*$^{-/-}$ embryos at E14.5. (C to F) Col10a1 appears in the region of hypertrophic chondrocytes at E14.5 (C and D) and then declines in the most mature hypertrophic chondrocytes at the center of hypertrophic zones at E15.5 in both groups without an apparent difference between wild-type and mutant embryos (E and F). Scale bars, 200 μm.

and 5′-GGGCGGTACTCAGAACAGAA (antisense); and GAPDH, 5′-ATGT GTCCGTCGTGGATCTGA (sense) and 5′-GATGCCTGCTTCACCACCTT (antisense).

Statistics. The statistical analysis at present study was performed by using a two-tailed Student *t* test.

RESULTS

Analysis of skeletal development in *Hmgb1*$^{-/-}$ mice. We first examined bone and cartilage development in *Hmgb1*$^{-/-}$ mice. Since *Hmgb1*$^{-/-}$ mice die soon after birth (11), we analyzed *Hmgb1*$^{-/-}$ embryos. Alcian blue staining revealed no apparent difference in skeletal formation between *Hmgb1*$^{-/-}$ and wild-type littermate embryos at E13.5 (see Fig. S1A in the supplemental material). At E16.5, however, *Hmgb1*$^{-/-}$ embryos were smaller than wild-type embryos, suggesting a discrepancy during ossification (Fig. 1A). At this stage, facial and skull bones formed by intramembranous ossification appeared similar between the two groups, although the shape of *Hmgb1*$^{-/-}$ calvariae was relatively flat and depressed. In contrast, sphenoid bones and the basioccipital region of the chondrocranium, which are formed by endochondral ossification, appeared to be reduced in size and in intensity of alizarin red staining in *Hmgb1*$^{-/-}$ mice (Fig. 1B). Other bones formed by endochondral ossification, such as the pelvis, had smaller alizarin red-stained zones (Fig. 1C). The radius and ulna of *Hmgb1*$^{-/-}$ forelimbs were not only reduced in size and calcification but abnormally bent, suggesting a reduction of mineralization (Fig. 1D). Moreover, fractures were observed in the humeri of some (4 of 14) *Hmgb1*$^{-/-}$ mice. Thorax formation showed severe hypoplasia accompanied by spinal scoliosis (Fig. 1E) and kyphosis (Fig. 1A). Ribs stained less intensely for alizarin red and were thin and bent (Fig. 1F). The clavicles were hypoplastic and crooked (Fig. 1G). At E16.5, the diameters of calvariae were similar in both groups, whereas the lengths of the *Hmgb1*$^{-/-}$ tibias reached 87% of that of the wild type, and the alizarin-positive region reached 64% of the wild-type length (Fig. 1H). These findings suggest that in *Hmgb1*$^{-/-}$ mice endochondral ossification is impaired, whereas intramembranous ossification is only affected slightly and was not investigated further.

HMGB1 expression in normal growth plates. To investigate the mechanism of endochondral ossification defect in *Hmgb1*$^{-/-}$ embryos, we examined the localization of HMGB1 protein in the developing limbs of normal wild-type mice by immunohistochemistry. Safranin O staining showed that prehypertrophic cartilage appeared in the tibia at E14.5 (Fig. 2A), differentiating into hypertrophic cartilage, followed by calcified cartilage at E15.5 (Fig. 2C), and was replaced by bone marrow and bone trabeculae at E16.5 (Fig. 2E). By using the specific anti-HMGB1 polyclonal rabbit antibody which does not detect HMGB2 and HMGB3 (19), we found that HMGB1 was expressed in the prehypertrophic chondrocytes of the tibia at E14.5 (Fig. 2B) and in hypertrophic chondrocytes at E15.5 (Fig. 2D). Large magnifications of the humerus at E15.5 showed that HMGB1 was detected in the nuclei of prehypertrophic chondrocytes and in the cytosol of hypertrophic chondrocytes (Fig. 2G). On the other hand, resting and proliferating chondrocytes did not show any positive staining in either nuclei or cytoplasm. Not only large long bones but also other small long bones formed by endochondral ossification, such as metacarpal bones, exhibited HMGB1 expression in the nuclei of prehypertrophic chondrocytes, as well as in the cytoplasm of hypertrophic chondrocytes (Fig. 2H). This positive staining in hypertrophic cartilage was absent in *Hmgb1*$^{-/-}$ sections (Fig. 2I). These results indicate that HMGB1 is expressed and translocated from the nucleus to the cytosol during a specific stage of cartilage maturation. At the end of the cascade of chondrocyte maturation, terminal hypertrophic chondrocytes undergo apoptotic cell death (17). We analyzed HMGB1 expression and apoptosis in the radius at E15.5 and detected HMGB1 in hypertrophic chondrocytes (Fig. 2J) but not in terminal hypertrophic chondrocytes, which were positive for TUNEL staining

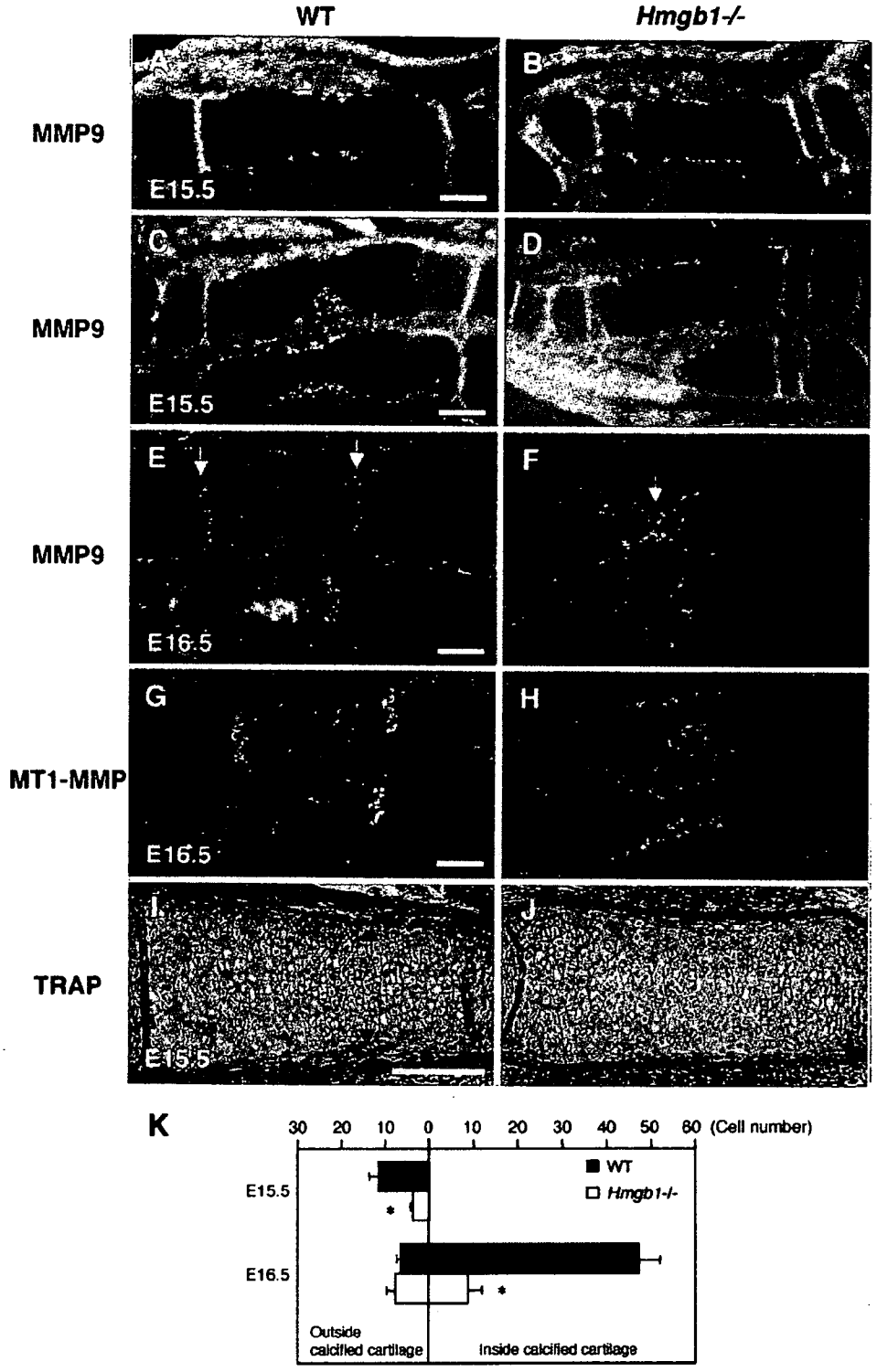

FIG. 4. Analysis of osteoclast markers in the primary ossification center. MMP9-positive osteoclastic cells are present in the perichondrium of the tibia (A) and radius and ulna (C) of wild-type embryos at E15.5 but are barely found in *Hmgb1*$^{-/-}$ bones (B and D). At E16.5, MMP9-positive cells are lining the transverse septae of cartilage-bone junctions that lead the vascular invasion front in wild-type radius (E, arrows), while they are still located in the primary ossification center in *Hmgb1*$^{-/-}$ bone (F, arrow). (G and H) The expression of MT1-MMP is similar to that of MMP9 in forelimbs at E16.5. TRAP staining indicates a significant reduction in the number of TRAP-positive cells in *Hmgb1*$^{-/-}$ tibia (J) compared to wild-type bone (I, arrows) at E15.5. (K) Quantification of the number of TRAP-positive cells in wild-type and *Hmgb1*$^{-/-}$ tibias. The total numbers of embryos were as follows: at E15.5, four wild-type and three mutant (pool of two littermates); and at E16.5, four wild-type and three mutant (pool of three littermates). The horizontal bars show the mean counts of TRAP-positive cells found either outside the calcified hypertrophic cartilage at the perichondrium-periosteum or inside the calcified hypertrophic cartilage. In both stages, there is a significant difference in the total number of TRAP-positive cells between wild-type and *Hmgb1*$^{-/-}$ mice (*, $P < 0.01$). Scale bars, 200 μm.

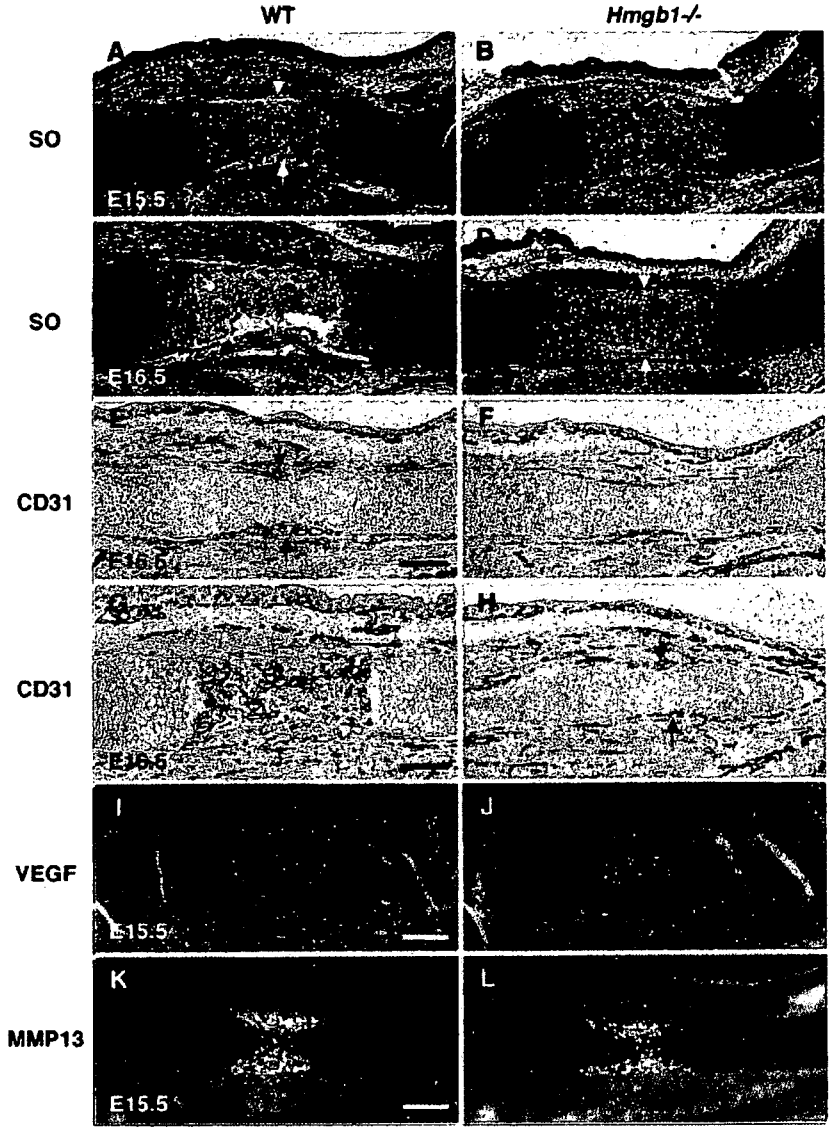

FIG. 5. Comparison of vascularization in wild-type and *Hmgb1*$^{-/-}$ skeletal elements during development. Safranin O staining (SO) of E15.5 tibias reveals that blood vessel invasion into the hypertrophic zone occurs in wild-type mice (A, arrows) but not in *Hmgb1*$^{-/-}$ mice (B). (C) At E16.5, hypertrophic cartilage is replaced by bone marrow and bone trabeculae in wild-type mice. (D) In contrast, the primary ossification center of *Hmgb1*$^{-/-}$ tibia is still intact with a wide hypertrophic zone (arrowheads) at the onset of blood vessel invasion (arrows). CD31 immunostaining shows that blood vessels start to invade the hypertrophic zone of wild-type tibia at E15.5 (E, arrows), but they are only surrounding the surface of *Hmgb1*$^{-/-}$ tibia (F). At E16.5, blood vessels have fully penetrated into the primary ossification center and distribute in bone marrow in wild-type tibia (G), whereas they still only surround the hypertrophic cartilage in *Hmgb1*$^{-/-}$ tibia (H, arrows). (I and J) VEGF expression in hypertrophic cartilage is similar for wild-type and *Hmgb1*$^{-/-}$ tibias at E15.5. (K and L) MMP13 expression in the calcified cartilage of wild-type tibia also resembles that of *Hmgb1*$^{-/-}$ tibias at E15.5. Scale bars, 200 μm.

(Fig. 2K), suggesting that HMGB1 was expressed just before cell death.

Impaired invasion of osteoclasts in *Hmgb1*$^{-/-}$ mice. Next, we sought to identify which process during endochondral ossification was disturbed by *Hmgb1* gene deficiency. To examine the rate of hypertrophic chondrocyte differentiation, we observed the expression of Indian hedgehog, a marker of prehypertrophic chondrocytes of cartilage elements (52), and found that it did not differ between wild-type (Fig. 3A) and *Hmgb1*$^{-/-}$ (Fig. 3B) tibias. Col10a1 appeared in the region of hypertrophic chondrocytes at E14.5 (Fig. 3C and D) and then declined in the most mature hypertrophic chondrocytes at the center of hypertrophic zones at E15.5 with a similar pattern in both groups (Fig. 3E and F). These findings indicate that *Hmgb1* gene deficiency does not affect the onset of cartilage maturation. In contrast, MMP9-positive osteoclastic cells (53) were distributed around the perichondrium in the tibias and radii of wild-type mice at E15.5 (Fig. 4A and C) but were barely detectable in *Hmgb1*$^{-/-}$ bones (Fig. 4B and D). At E16.5, the discrepancy became more remarkable. In the wild-

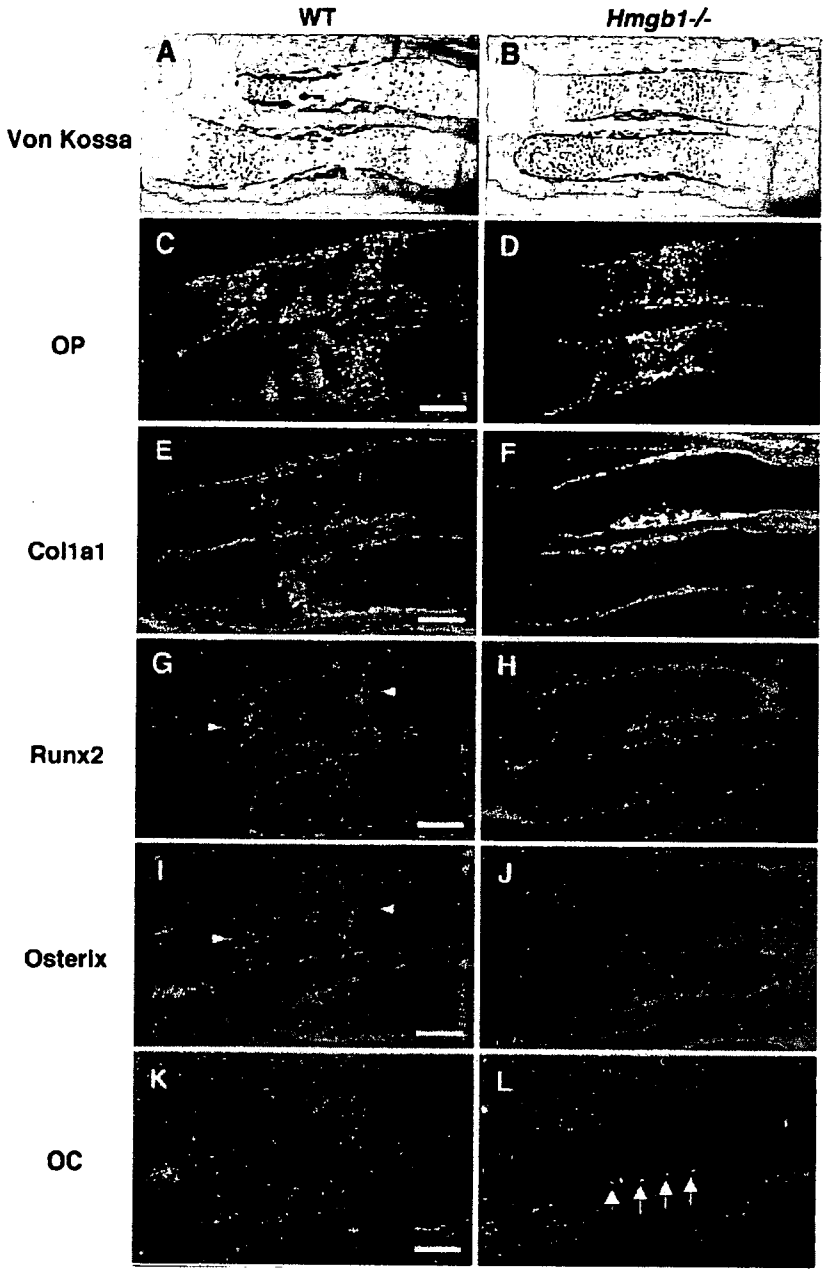

FIG. 6. Osteoblast differentiation markers in *Hmgb1*$^{-/-}$ forelimbs at E16.5. Von Kossa staining shows that calcified cartilage has not progressed to bone marrow in the radii and ulnas of *Hmgb1*$^{-/-}$ embryos (B) compared to wild-type embryos (A). Osteopontin (OP) is strongly expressed in the calcified hypertrophic cartilage of *Hmgb1*$^{-/-}$ bones (D), in which Col1a1-positive cells are not found (F). (C and E) In contrast, these osteoblastic cells are widely distributed in the bone marrow of wild-type bones. Runx2 and Osterix are highly expressed in the primary ossification center in wild-type radius (G and I, arrowheads), although they are barely detectable in *Hmgb1*$^{-/-}$ bones (H and J). Osteocalcin (OC) is found at the periphery of hypertrophic cartilage in *Hmgb1*$^{-/-}$ bones (L, arrows), while it appears in bone marrow in wild-type mice at E16.5 (K). Scale bars, 200 μm.

type radius, MMP9-positive cells were lining the transverse septae of cartilage-bone junctions that lead the vascular invasion front (Fig. 4E), whereas they were still located in the primary ossification center in *Hmgb1*$^{-/-}$ radius (Fig. 4F). The expression of MT1-MMP, which is highly expressed in osteoclasts (44), was similar to that of MMP9 (Fig. 4G and H). To confirm the apparent reduction in osteoclast numbers, we stained for TRAP and found significant reduction in the number of TRAP-positive cells in *Hmgb1*$^{-/-}$ tibias at E15.5 (Fig. 4I and J). Quantification of the number of these cells inside versus outside the calcified hypertrophic cartilage showed a significant difference between wild-type and *Hmgb1*$^{-/-}$ tibias (Fig. 4K). These findings demonstrate that osteoclast recruitment was suppressed in the *Hmgb1*$^{-/-}$ bones.

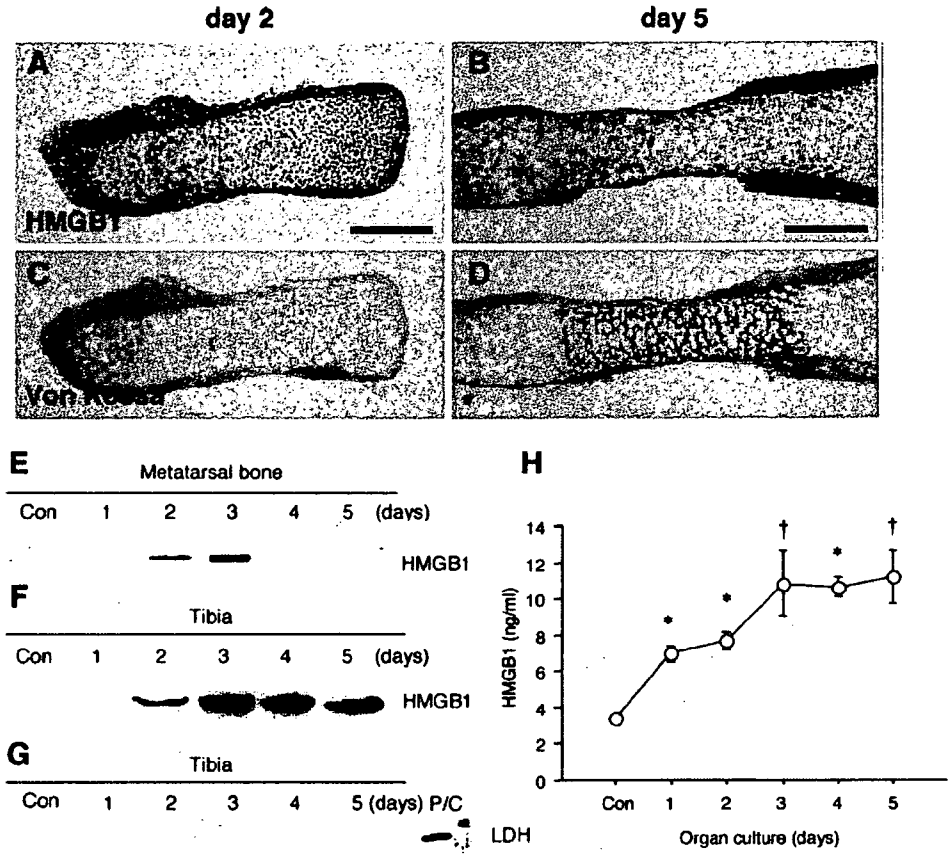

FIG. 7. HMGB1 is released extracellularly by developing cartilage. Metatarsal bones were isolated from wild-type embryos at E15.5 and cultured for up to 5 days. Immunohistochemistry reveals that HMGB1 is localized in hypertrophic chondrocytes of metatarsal bones on day 2 (A) and that expression is attenuated on day 5 (B). (C and D) Von Kossa staining with the adjacent sections shows that HMGB1 expression occurs in hypertrophic cartilage and not in calcified cartilage. Scale bars, 200 μm. Immunoblotting was carried out to determine the release of HMGB1 by cultured metatarsal bones. (E) HMGB1 is present in the supernatant with a peak 3 days after the start of organ culture, and then it decreases. (F) A large long bone, the tibia, which was isolated from embryos at E14.5, also releases HMGB1 in the supernatant. (G) The supernatant of the tibia does not contain LDH, a marker for cell necrosis; mouse rib chondrocytes undergoing necrosis are used as a positive control (P/C). (H) The HMGB1 level in the supernatant of tibia organ culture was quantified by ELISA. HMGB1 is released in a time-dependent fashion, which peaked on days 3, 4, and 5 at concentrations of 10.8 ± 5.4, 10.7 ± 1.6. and 11.2 ± 4.4 ng/ml, respectively. Statistically significant differences from the HMGB1 level in control supernatant are indicated (*, $P < 0.01$; †, $P < 0.05$).

Altered vascularization of skeletal elements in *Hmgb1*$^{-/-}$ mice during development. MMP9-positive cells enter the mesenchyme surrounding the bone rudiments and migrate together with endothelial cells through the nascent bone collar at the primary ossification center (15). Thus, we examined the vascularization in skeletal elements of *Hmgb1*$^{-/-}$ mice. Safranin O staining revealed that blood vessel invasion into the hypertrophic zone occurred in wild-type tibias at E15.5 (Fig. 5A) but not in *Hmgb1*$^{-/-}$ tibias (Fig. 5B). At E16.5, hypertrophic cartilage was replaced by bone marrow and bone trabeculae in wild-type mice (Fig. 5C). In contrast, the primary ossification center of *Hmgb1*$^{-/-}$ tibias was still intact with a wide hypertrophic zone and only the onset of blood vessel invasion (Fig. 5D). Using CD31 (PECAM) antibody, which is a marker of endothelial cells, we performed immunostaining and found that blood vessels started to invade the hypertrophic zone of wild-type tibia at E15.5 (Fig. 5E), but they were only on the surface of *Hmgb1*$^{-/-}$ tibia (Fig. 5F). At E16.5, blood vessels had fully penetrated into the primary ossification center and distributed in bone marrow in wild-type tibia (Fig. 5G), whereas they were still only surrounding the hypertrophic cartilage in *Hmgb1*$^{-/-}$ bone (Fig. 5H). At the growth plate, hypertrophic cartilage expresses VEGF, and inhibition of VEGF activity blocks the recruitment of MMP9-positive and TRAP-positive cells, as well as endothelial cells (17). We found no difference in VEGF expression in hypertrophic cartilage between wild-type and *Hmgb1*$^{-/-}$ tibia at E15.5 (Fig. 5I and J). MMP13, which is expressed by both terminal hypertrophic chondrocytes and osteoblasts, is also important for the vascularization of hypertrophic cartilage because it degrades native collagen, a major component of the hypertrophic cartilage (47). MMP13 expression in the calcified cartilage of the wild-type tibia resembled that of the *Hmgb1*$^{-/-}$ tibia (Fig. 5K and L). Taken together, these findings suggest that the cell invasion into hypertrophic cartilage by endothelial cells was disrupted in *Hmgb1*$^{-/-}$ bones during the process of endochondral ossification, although VEGF and MMP13 expression was unaltered.

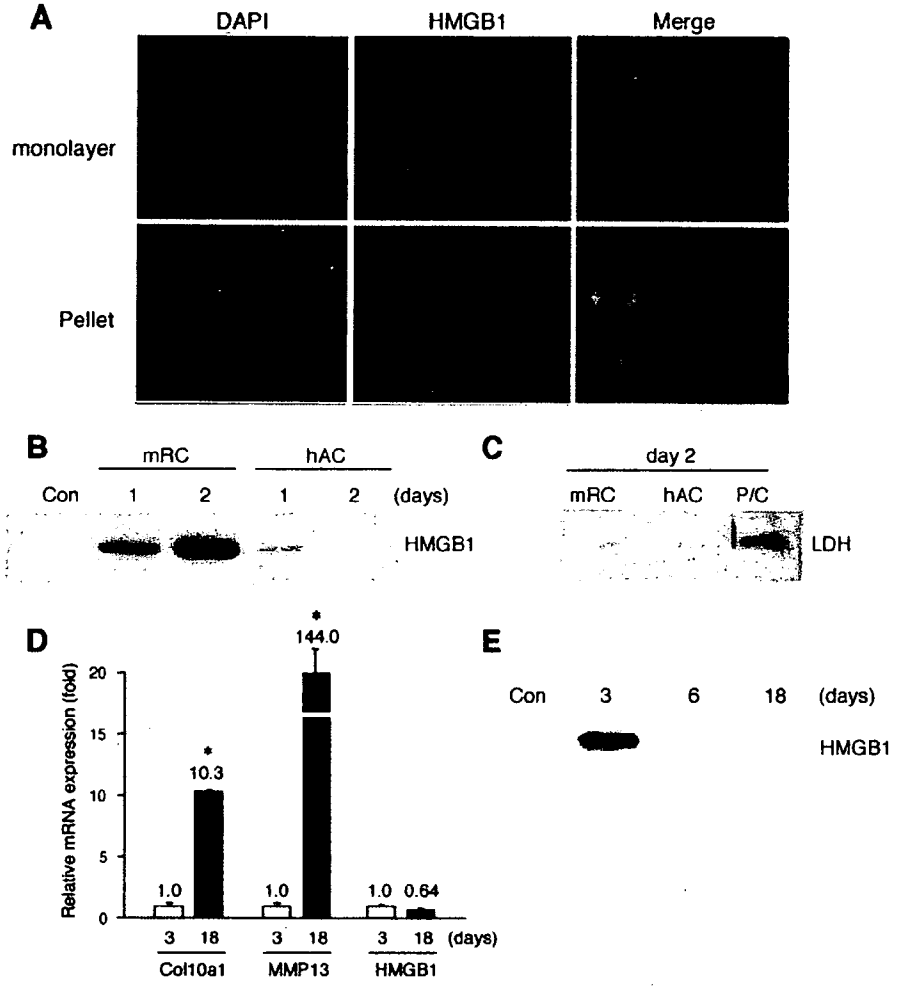

FIG. 8. HMGB1 release from differentiating cultured rib chondrocytes. (A) Immunofluorescence assay shows that monolayer rib chondrocytes isolated from the ventral parts of mice rib cartilage express HMGB1 only in the nucleus, whereas in pelleted rib chondrocytes cultured for 2 days HMGB1 is localized in the cytosol. The extracellular release of HMGB1 was verified with immunoblotting. (B) HMGB1 was determined in the supernatant of pelleted mice rib chondrocytes (mRC) on days 1 and 2, whereas human articular chondrocytes (hAC) do not release HMGB1 in pellet culture. (C) Immunoblotting with LDH antibody shows that this secretion is independent of necrotic cell death. The positive control (P/C) is the same sample as shown in Fig. 7G. (D) During the culture of pelleted mRC for 18 days, quantitative PCR demonstrates that the mRNA level of cartilage maturation markers such as Col10a1 and MMP13 increases significantly on day 18, although that of HMGB1 is unchanged. (E) Only the supernatant on day 3 contains HMGB1. Statistically significant differences from mRNA expression on day 3 are indicated, respectively (*, $P < 0.01$).

Osteogenesis in *Hmgb1*$^{-/-}$ mice. As shown in Fig. 1, *Hmgb1*$^{-/-}$ forelimbs appeared to be reduced in size and calcification and were abnormally bent or fractured. Since these findings suggest a reduction of bone mineralization, we investigated osteoblast differentiation in *Hmgb1*$^{-/-}$ bones. Using von Kossa staining, we found that calcified cartilage had progressed to bone marrow in the radii and ulnas of wild-type mice (Fig. 6A) but not in *Hmgb1*$^{-/-}$ mice (Fig. 6B). Osteopontin, a hypertrophic cartilage marker as well as an osteoblast marker (35), was strongly expressed in the calcified hypertrophic cartilage of *Hmgb1*$^{-/-}$ bones (Fig. 6D) in which Col1a1-positive cells, an early marker of osteoblast differentiation (18), were not found; these cells were accumulated at the collar surrounding the growth plate (Fig. 6F). In contrast, Col1a1-positive cells were widely distributed in the bone marrow of wild-type mice (Fig. 6E), suggesting that osteoblast invasion was suppressed in *Hmgb1*$^{-/-}$ limbs. The essential transcription factors for osteoblast differentiation, Runx2 (27) and Osterix (34), were highly expressed in the primary ossification center of the wild-type radius (Fig. 6G and I), whereas they were barely detectable in the *Hmgb1*$^{-/-}$ bones (Fig. 6H and J). Osteocalcin, which is thought to be a terminal marker for osteoblastic maturation (29), was found at the periphery of hypertrophic cartilage in *Hmgb1*$^{-/-}$ bones at E16.5 (Fig. 6L); however, it appeared in the bone marrow at E17.5 (data not shown) rather than at E16.5 as in wild-type mice (Fig. 6K). Thus, the delay in primary ossification of *Hmgb1*$^{-/-}$ hypertrophic cartilage was coupled to a delay in recruitment of osteoblasts, suggesting that subsequent osteoblastic differentiation progressed similarly in wild-type and *Hmgb1*$^{-/-}$ mice.

HMGB1 is released from differentiating cartilage in organ culture. To examine the secretion of HMGB1 from chon-

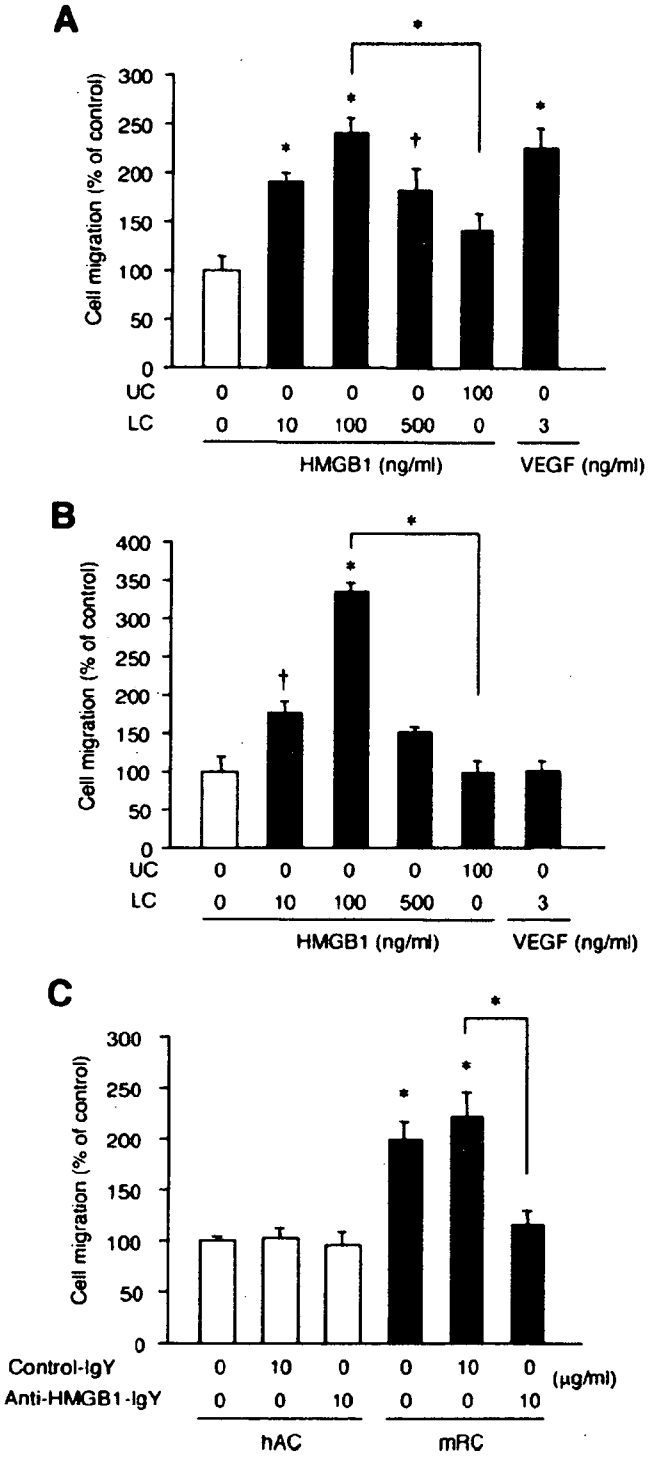

FIG. 9. Chondrocyte-secreted HMGB1 is a chemoattractant for osteoclasts. The chemotactic effect of recombinant HMGB1 on osteoclasts was examined by Boyden chambers with or without addition of HMGB1 to either the lower chamber (LC) or the upper chamber (UC) as indicated. (A) HMGB1 recruits osteoclasts at 10 ng/ml, and efficacy peaks at 100 ng/ml. The addition of HMGB1 to the upper chamber does not significantly activate osteoclast invasion. (B) HMGB1 also recruits osteoblastic MC3T3-E1 cells with a tendency similar to that described above, although VEGF does not. Statistically significant differences from control migrations without added chemoattractants are indicated, respectively (*, $P < 0.01$; †, $P < 0.05$). (C) Chemotaxis assay using the supernatant of pelleted mice rib chondrocytes (mRC) and human articular chondrocytes (hAC) after 3 days culture. The supernatant of hAC does not recruit osteoclasts, whereas that of mRC attracts osteoclasts significantly, and this effect is abrogated by addition of anti-HMGB1 IgY. Cell migration is shown as mean ± the standard deviation of four replicates. Statistically significant differences from control migrations by the supernatant of hAC are indicated (*, $P < 0.01$).

drocytes, we used the cartilage organ culture system (20). Metatarsal bones were isolated from embryos at E15.5 and cultured in conditioned medium for up to 5 days. Immunohistochemistry revealed that HMGB1 was localized in hypertrophic chondrocytes on day 2 (Fig. 7A) and that expression was attenuated on day 5 (Fig. 7B). Von Kossa staining of the adjacent sections indicated that this expression occurred in hypertrophic cartilage and not in calcified cartilage (Fig. 7C and D). Using immunoblotting, we determined that HMGB1 was present in the supernatant, with a peak 3 days after the start of organ culture, and then it decreased (Fig. 7E), showing that HMGB1 was released into the medium by hypertrophic chondrocytes. This result was reproduced with a large long bone, the tibia, which was isolated from the embryos at E14.5 (Fig. 7F). Immunoblotting with LDH antibody was negative, indicating that HMGB1 was actively secreted and not released passively as a consequence of necrotic cell death (Fig. 7G). Using ELISA, we quantified the HMGB1 protein released into the medium of tibia organ culture and found that it peaked on days 3 through 5 at concentrations of >10 ng/ml (Fig. 7H).

HMGB1 is released specifically from hypertrophic chondrocytes. It has been previously demonstrated that HMGB1 is released from osteoclasts and osteoblast-like cells (12, 42). To prove that the release of HMGB1 into the supernatant was from chondrocytes in organ culture, we used pellet cultures of rib growth plate chondrocytes, since this culture system mimics in vivo cartilage differentiation (5). Monolayer chondrocytes isolated from the ventral parts of mouse rib cartilage expressed HMGB1 only in the nucleus; however, when cultured as differentiating cell pellets, HMGB1 was localized in the cytosol (Fig. 8A). Extracellular HMGB1 was detected in the supernatant of pelleted rib chondrocytes on days 1 and 2; in contrast, articular chondrocytes, which do not differentiate to hypertrophic cartilage under the three-dimensional condition such as pellet or alginate culture (6, 40), did not release HMGB1 (Fig. 8B). Immunoblotting with LDH antibody showed that HMGB1 release was not caused by necrotic cell death (Fig. 8C). In addition, to examine HMGB1 expression in longer-term cultures, we maintained the rib chondrocyte pellets for 18 days. Quantitative PCR demonstrated that mRNA of cartilage maturation markers such as Col10a1 and MMP13 increased significantly, showing that chondrocyte differentiation had occurred (Fig. 8D). Only the medium from day 3 contained HMGB1 (Fig. 8E), although the mRNA level of HMGB1 did not significantly change between day 3 and 18. These results indicate that HMGB1 is secreted during the early phase of cartilage maturation.

HMGB1 is a chemoattractant for osteoclasts and osteoblasts. As we showed in Fig. 4, 5, and 6, *Hmgb1*$^{-/-}$ embryos

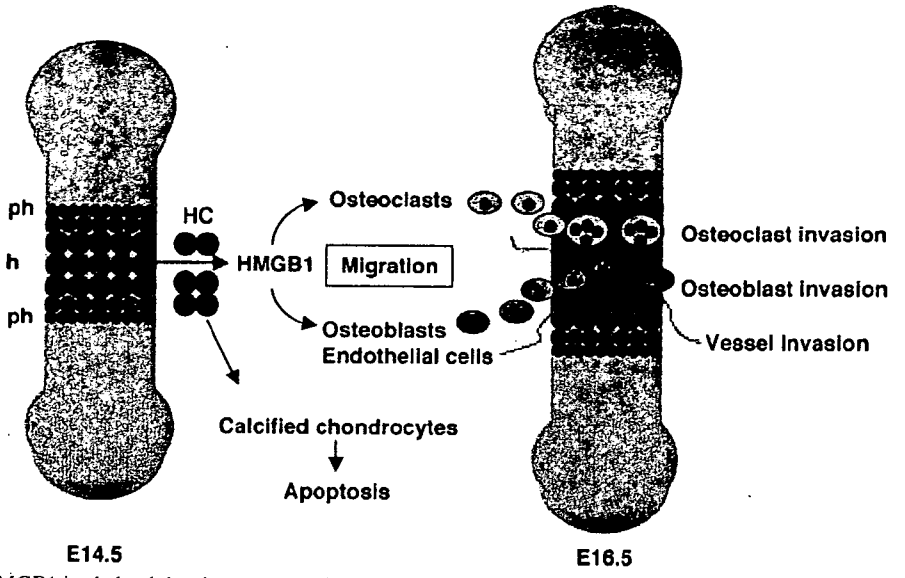

FIG. 10. Role of HMGB1 in skeletal development. During endochondral ossification, a region of resting chondrocytes transforms into a zone of proliferating chondrocytes that then undergo hypertrophy and subsequently apoptosis. HMGB1 is released from the hypertrophic chondrocytes just before undergoing programmed cell death; it acts as an extracellular signal for the migration of osteoclasts, osteoblasts, and endothelial cells that replace cartilage with bone and bone marrow. ph, prehypertrophic cartilage; h, hypertophic cartilage; bm, bone marrow; HC, hypertrophic chondrocytes.

were defective in invasion by TRAP- and Col1a1-positive cells, as well as CD31-positive cells, at the primary ossification center. Since HMGB1 has chemotactic effects on endothelial cells (32, 46), we tested for similar effects on osteoclasts and osteoblasts. Recombinant HMGB1 at 10 ng/ml recruited osteoclasts in Boyden chambers, and peak migration occurred at 100 ng/ml; this level of efficacy was similar to that of VEGF used as a positive control (22) (Fig. 9A). Addition of HMGB1 to the upper chamber did not significantly activate osteoclast migration. HMGB1 also induced chemotaxis for MC3T3-E1 osteoblast-like cells with a tendency similar to that described above (Fig. 9B), although VEGF did not (16). These findings suggest that osteoclast and osteoblast invasion at the primary ossification center might be a direct effect of HMGB1-induced chemoattraction.

Finally, we investigated whether HMGB1 released by differentiating chondrocytes could promote osteoclast migration. Using the supernatant of pelleted rib chondrocytes and articular chondrocytes cultured for 3 days (see Fig. S2 in the supplemental material), we compared the chemotactic effect for osteoclasts. The supernatant of articular chondrocytes did not recruit osteoclasts; however, the supernatant of rib chondrocytes attracted osteoclasts significantly, and the effect was abrogated by neutralizing anti-HMGB1 IgY (Fig. 9C). This result supports our hypothesis that differentiating chondrocytes could regulate cell migration directly via HMGB1 secretion.

DISCUSSION

This study demonstrates that the stage-specific secretion of HMGB1 in cartilage regulates endochondral ossification, at least in part, by acting as a chemotactic factor for osteoclasts and osteoblasts, as well as endothelial cells. We examined skeletal development in *Hmgb1*$^{-/-}$ embryos and found significant alterations in the bones formed by endochondral ossification, whereas calvariae, which are formed by intramembranous ossification, were somewhat misshapen, but the effect was slight, and the cartilage formation was not affected. The analysis of *Hmgb1*$^{-/-}$ limb sections revealed that the onset of cartilage differentiation was similar in *Hmgb1*$^{-/-}$ and wild-type embryos; however, the invasion of TRAP- and Col1a1-positive cells, as well as CD31-positive cells, into the primary ossification center was remarkably impaired in *Hmgb1*$^{-/-}$ limbs. Thus, the *Hmgb1*$^{-/-}$ growth plates are strikingly lengthened and deficient in osteoblast and osteoclast invasion as well as vascularization, which may result in weak bones that can bend or fracture.

To examine the expression of HMGB1 in developing limbs, we used in situ hybridization: HMGB1 mRNA expression was ubiquitous in the cells of all zones of the growth plate from E14.5 through E16.5 (data not shown). In contrast, HMGB1 protein was present in the nuclei of prehypertrophic chondrocytes in tibia at E14.5 and in the cytosol of hypertrophic chondrocytes at E15.5 but was not detectable in resting and proliferating chondrocytes. The active secretion of HMGB1 from chondrocytes was verified with organ culture and pellet culture systems; we found that HMGB1 was translocated from the nucleus to the cytosol and actively secreted at the early phase of chondrocyte differentiation, but the secretion ceased at the late phase. Interestingly, secretion from pelleted rib chondrocytes occurred actively without added any stimulatory factor, whereas articular chondrocytes did not release HMGB1 in pellet culture. Chondrocyte-secreted HMGB1 was sufficient to chemoattract osteoclasts and osteoblasts, as well as endothelial cells as previously shown by others (32, 46). These findings suggest that HMGB1 released from hypertrophic chondrocytes may regulate skeletal development by controlling cell invasion

into the growth plate. At present, however, a potential role of HMGB1 as a nuclear factor, which is its other function, still remains possible in the developing cartilage.

Secretion of HMGB1 during specific stages of cell differentiation is not unique to chondrocytes and has been reported for dendritic cells (14) and neonatal rat type I astrocytes (41), although the mechanism of HMGB1 secretion during cell differentiation has yet to be elucidated. Thus far, Bonaldi et al. have reported that HMGB1 contains two nuclear localization signals (NLSs), and the acetylation of both NLSs is involved in the transport from the nucleus to the cytosol (8). Furthermore, HMGB1 can be phosphorylated, and the direction of transport is regulated by phosphorylation of both NLS regions (58). These findings suggest that HMGB1 release is independent from RNA expression and protein synthesis, which is compatible with our data showing that HMGB1 mRNA levels do not change in chondrocyte pellet cultures, despite its secretion.

The inhibition of the interaction between HMGB1 and the receptor for advanced glycation end products (RAGE), which is a specific receptor for HMGB1, suppresses the tumor proliferation, metastatic invasion, and expression of MMPs (48). RAGE is expressed in osteoclasts, osteoblasts (12), and endothelial cells (9), suggesting that RAGE might be associated with cell invasion during endochondral ossification; however, an analysis of *Rage*$^{-/-}$ mice (1) showed no alteration in skeletal development during embryogenesis (see Fig. S1B in the supplemental material). Moreover, *Rage*$^{-/-}$ mice manifest increased bone mass and bone mineral density and decreased bone resorptive activity due to a defect in osteoclast function (60). In our hands, however, MMP9 mRNA levels in calvariae at E18.5 were similar between wild-type and *Hmgb1*$^{-/-}$ mice (see Fig. S3A in the supplemental material), and MMP9-positive cells emerged in the bone marrow of developing limbs of both types of mice at E18.5 (see Fig. S3B in the supplemental material). The evidence that HMGB1-RAGE interaction is sufficient but not necessary for mesoangioblast migration (38) is a precedent for the idea that RAGE may not be the key receptor for HMGB1-induced cell recruitment at the primary ossification center. Additional HMGB1 receptors have been identified, including Toll-like receptors 2 and 4 (39), which appear in osteoclasts, osteoblasts, and endothelial cells (26, 49, 50), and syndecan (43), which is expressed in osteoblasts (24).

Our results indicate that HMGB1 might be important not only for tissue repair after injury but also for the organization of bone and cartilage development in the embryo. In endochondral ossification, a region of resting chondrocytes transforms into a zone of proliferating chondrocytes that then undergo hypertrophy and subsequently apoptosis (37). HMGB1 release from the hypertrophic cartilage occurs just before programmed cell death (Fig. 10), suggesting that HMGB1 may be an extracellular signal released from the tissue to be replaced (cartilage) toward the cells of new tissue to be formed (bone and bone marrow).

ACKNOWLEDGMENTS

We are grateful to Yasuhiko Kawakami and Thiennu Vu for helpful discussions; Kim Henriksen, Noriyuki Namba, and Chisa Shukunami for technical advice; Yasuhiko Yamamoto and Hiroshi Yamamoto for providing *Rage*$^{-/-}$ mice; and Shingo Yamada for providing the neutralizing anti-HMGB1 IgY and ELISA kit. We especially thank Lilo Creighton for her excellent immunohistochemical technique.

This study was supported by grants from the NIH (AR47360, AR50631, and AG07996), NIBI (ID05-24), Arthritis Foundation, JST SORST, Genome Network Project (MEXT), and Grants-in Aid for Scientific Research (MEXT) (H.A.) and a postdoctoral fellowship of the Japan Research Foundation for Clinical Pharmacology and Research Grant for Rheumatology Disease, Japan Rheumatism Foundation (N.T.).

REFERENCES

1. **Abeyama, K., D. M. Stern, Y. Ito, K. Kawahara, Y. Yoshimoto, M. Tanaka, T. Uchimura, N. Ida, Y. Yamazaki, S. Yamada, Y. Yamamoto, H. Yamamoto, S. Iino, N. Taniguchi, and I. Maruyama.** 2005. The N-terminal domain of thrombomodulin sequesters high-mobility group-B1 protein, a novel antiinflammatory mechanism. J. Clin. Investig. **115**:1267–1274.
2. **Agresti, A., and M. E. Bianchi.** 2003. HMGB proteins and gene expression. Curr. Opin. Genet. Dev. **13**:170–178.
3. **Albrecht, U., G. Eichele, J. A. Helms, and H. Lu.** 1997. Molecular and cellular methods in developmental toxicology. CRC Press, Boca Raton, FL.
4. **Andersson, U., H. Wang, K. Palmblad, A. C. Aveberger, O. Bloom, H. Erlandsson-Harris, A. Janson, R. Kokkola, M. Zhang, H. Yang, and K. J. Tracey.** 2000. High mobility group 1 protein (HMG-1) stimulates proinflammatory cytokine synthesis in human monocytes. J. Exp. Med. **192**:565–570.
5. **Ballock, R. T., and A. H. Reddi.** 1994. Thyroxine is the serum factor that regulates morphogenesis of columnar cartilage from isolated chondrocytes in chemically defined medium. J. Cell Biol. **126**:1311–1318.
6. **Binette, F., D. P. McQuaid, D. R. Haudenschild, P. C. Yaeger, J. M. McPherson, and R. Tubo.** 1998. Expression of a stable articular cartilage phenotype without evidence of hypertrophy by adult human articular chondrocytes in vitro. J. Orthop. Res. **16**:207–216.
7. **Blavier, L., and J. M. Delaisse.** 1995. Matrix metalloproteinases are obligatory for the migration of preosteoclasts to the developing marrow cavity of primitive long bones. J. Cell Sci. **108**(Pt. 12):3649–3659.
8. **Bonaldi, T., F. Talamo, P. Scaffidi, D. Ferrera, A. Porto, A. Bachi, A. Rubartelli, A. Agresti, and M. E. Bianchi.** 2003. Monocytic cells hyperacetylate chromatin protein HMGB1 to redirect it toward secretion. EMBO J. **22**: 5551–5560.
9. **Brett, J., A. M. Schmidt, S. D. Yan, Y. S. Zou, E. Weidman, D. Pinsky, R. Nowygrod, M. Neeper, C. Przysiecki, A. Shaw, et al.** 1993. Survey of the distribution of a newly characterized receptor for advanced glycation end products in tissues. Am. J. Pathol. **143**:1699–1712.
10. **Bustin, M.** 1999. Regulation of DNA-dependent activities by the functional motifs of the high-mobility-group chromosomal proteins. Mol. Cell. Biol. **19**:5237–5246.
11. **Calogero, S., F. Grassi, A. Aguzzi, T. Voigtlander, P. Ferrier, S. Ferrari, and M. E. Bianchi.** 1999. The lack of chromosomal protein Hmg1 does not disrupt cell growth but causes lethal hypoglycaemia in newborn mice. Nat. Genet. **22**:276–280.
12. **Charoonpatrapong, K., R. Shah, A. G. Robling, M. Alvarez, D. W. Clapp, S. Chen, R. P. Kopp, F. M. Pavalko, J. Yu, and J. P. Bidwell.** 2006. HMGB1 expression and release by bone cells. J. Cell Physiol. **207**:480–490.
13. **Degryse, B., T. Bonaldi, P. Scaffidi, S. Muller, M. Resnati, F. Sanvito, G. Arrigoni, and M. E. Bianchi.** 2001. The high mobility group (HMG) boxes of the nuclear protein HMG1 induce chemotaxis and cytoskeleton reorganization in rat smooth muscle cells. J. Cell Biol. **152**:1197–1206.
14. **Dumitriu, I. E., P. Baruah, B. Valentinis, R. E. Voll, M. Herrmann, P. P. Nawroth, B. Arnold, M. E. Bianchi, A. A. Manfredi, and P. Rovere-Querini.** 2005. Release of high mobility group box 1 by dendritic cells controls T-cell activation via the receptor for advanced glycation end products. J. Immunol. **174**:7506–7515.
15. **Engsig, M. T., Q. J. Chen, T. H. Vu, A. C. Pedersen, B. Therkidsen, L. R. Lund, K. Henriksen, T. Lenhard, N. T. Foged, Z. Werb, and J. M. Delaisse.** 2000. Matrix metalloproteinase 9 and vascular endothelial growth factor are essential for osteoclast recruitment into developing long bones. J. Cell Biol. **151**:879–889.
16. **Fukuyama, R., T. Fujita, Y. Azuma, A. Hirano, H. Nakamuta, M. Koida, and T. Komori.** 2004. Statins inhibit osteoblast migration by inhibiting Rac-Akt signaling. Biochem. Biophys. Res. Commun. **315**:636–642.
17. **Gerber, H. P., T. H. Vu, A. M. Ryan, J. Kowalski, Z. Werb, and N. Ferrara.** 1999. VEGF couples hypertrophic cartilage remodeling, ossification and angiogenesis during endochondral bone formation. Nat. Med. **5**:623–628.
18. **Gerstenfeld, L. C., S. D. Chipman, J. Glowacki, and J. B. Lian.** 1987. Expression of differentiated function by mineralizing cultures of chicken osteoblasts. Dev. Biol. **122**:49–60.
19. **Guazzi, S., A. Strangio, A. T. Franzi, and M. E. Bianchi.** 2003. HMGB1, an architectural chromatin protein and extracellular signalling factor, has a spatially and temporally restricted expression pattern in mouse brain. Gene Expr. Patterns **3**:29–33.
20. **Haaijman, A., R. N. D'Souza, A. L. Bronckers, S. W. Goei, and E. H. Burger.** 1997. OP-1 (BMP-7) affects mRNA expression of type I, II, X collagen, and matrix Gla protein in ossifying long bones in vitro. J. Bone Miner. Res. **12**:1815–1823.

21. **Hashimoto, S., R. L. Ochs, F. Rosen, J. Quach, G. McCabe, J. Solan, J. E. Seegmiller, R. Terkeltaub, and M. Lotz.** 1998. Chondrocyte-derived apoptotic bodies and calcification of articular cartilage. Proc. Natl. Acad. Sci. USA **95**:3094–3099.
22. **Henriksen, K., M. Karsdal, J. M. Delaisse, and M. T. Engsig.** 2003. RANKL and vascular endothelial growth factor (VEGF) induce osteoclast chemotaxis through an ERK1/2-dependent mechanism. J. Biol. Chem. **278**:48745–48753.
23. **Holmbeck, K., P. Bianco, J. Caterina, S. Yamada, M. Kromer, S. A. Kuznetsov, M. Mankani, P. G. Robey, A. R. Poole, I. Pidoux, J. M. Ward, and H. Birkedal-Hansen.** 1999. MT1-MMP-deficient mice develop dwarfism, osteopenia, arthritis, and connective tissue disease due to inadequate collagen turnover. Cell **99**:81–92.
24. **Imai, S., M. Kaksonen, E. Raulo, T. Kinnunen, C. Fages, X. Meng, M. Lakso, and H. Rauvala.** 1998. Osteoblast recruitment and bone formation enhanced by cell matrix-associated heparin-binding growth-associated molecule (HB-GAM). J. Cell Biol. **143**:1113–1128.
25. **Inada, M., Y. Wang, M. H. Byrne, M. U. Rahman, C. Miyaura, C. Lopez-Otin, and S. M. Krane.** 2004. Critical roles for collagenase-3 (Mmp13) in development of growth plate cartilage and in endochondral ossification. Proc. Natl. Acad. Sci. USA **101**:17192–17197.
26. **Kikuchi, T., T. Matsuguchi, N. Tsuboi, A. Mitani, S. Tanaka, M. Matsuoka, G. Yamamoto, T. Hishikawa, T. Noguchi, and Y. Yoshikai.** 2001. Gene expression of osteoclast differentiation factor is induced by lipopolysaccharide in mouse osteoblasts via Toll-like receptors. J. Immunol. **166**:3574–3579.
27. **Komori, T., H. Yagi, S. Nomura, A. Yamaguchi, K. Sasaki, K. Deguchi, Y. Shimizu, R. T. Bronson, Y. H. Gao, M. Inada, M. Sato, R. Okamoto, Y. Kitamura, S. Yoshiki, and T. Kishimoto.** 1997. Targeted disruption of Cbfa1 results in a complete lack of bone formation owing to maturational arrest of osteoblasts. Cell **89**:755–764.
28. **Lefebvre, V., S. Garofalo, G. Zhou, M. Metsaranta, E. Vuorio, and B. De Crombrugghe.** 1994. Characterization of primary cultures of chondrocytes from type II collagen/beta-galactosidase transgenic mice. Matrix Biol. **14**: 329–335.
29. **Lian, J. B., G. S. Stein, C. Stewart, E. Puchacz, S. Mackowiak, M. Aronow, M. Von Deck, and V. Shalhoub.** 1989. Osteocalcin: characterization and regulated expression of the rat gene. Connect. Tissue Res. **21**:61–69.
30. **Liu, W., S. Toyosawa, T. Furuichi, N. Kanatani, C. Yoshida, Y. Liu, M. Himeno, S. Narai, A. Yamaguchi, and T. Komori.** 2001. Overexpression of Cbfa1 in osteoblasts inhibits osteoblast maturation and causes osteopenia with multiple fractures. J. Cell Biol. **155**:157–166.
31. **McLeod, M. J.** 1980. Differential staining of cartilage and bone in whole mouse fetuses by alcian blue and alizarin red S. Teratology **22**:299–301.
32. **Mitola, S., M. Belleri, C. Urbinati, D. Coltrini, B. Sparatore, M. Pedrazzi, E. Melloni, and M. Presta.** 2006. Cutting edge: extracellular high mobility group box-1 protein is a proangiogenic cytokine. J. Immunol. **176**:12–15.
33. **Nakashima, K., and B. de Crombrugghe.** 2003. Transcriptional mechanisms in osteoblast differentiation and bone formation. Trends Genet. **19**:458–466.
34. **Nakashima, K., X. Zhou, G. Kunkel, Z. Zhang, J. M. Deng, R. R. Behringer, and B. de Crombrugghe.** 2002. The novel zinc finger-containing transcription factor osterix is required for osteoblast differentiation and bone formation. Cell **108**:17–29.
35. **Nomura, S., A. J. Wills, D. R. Edwards, J. K. Heath, and B. L. Hogan.** 1988. Developmental expression of 2ar (osteopontin) and SPARC (osteonectin) RNA as revealed by in situ hybridization. J. Cell Biol. **106**:441–450.
36. **Okubo, Y., and A. H. Reddi.** 2003. Thyroxine downregulates Sox9 and promotes chondrocyte hypertrophy. Biochem. Biophys. Res. Commun. **306**:186–190.
37. **Ortega, N., D. J. Behonick, and Z. Werb.** 2004. Matrix remodeling during endochondral ossification. Trends Cell Biol. **14**:86–93.
38. **Palumbo, R., M. Sampaolesi, F. De Marchis, R. Tonlorenzi, S. Colombetti, A. Mondino, G. Cossu, and M. E. Bianchi.** 2004. Extracellular HMGB1, a signal of tissue damage, induces mesoangioblast migration and proliferation. J. Cell Biol. **164**:441–449.
39. **Park, J. S., D. Svetkauskaite, Q. He, J. Y. Kim, D. Strassheim, A. Ishizaka, and E. Abraham.** 2004. Involvement of Toll-like receptors 2 and 4 in cellular activation by high mobility group box 1 protein. J. Biol. Chem. **279**:7370–7377.
40. **Park, K., B. H. Min, D. K. Han, and K. Hasty.** 2007. Quantitative analysis of temporal and spatial variations of chondrocyte behavior in engineered cartilage during long-term culture. Ann. Biomed. Eng. **35**:419–428.
41. **Passalacqua, M., M. Patrone, G. B. Picotti, M. Del Rio, B. Sparatore, E. Melloni, and S. Pontremoli.** 1998. Stimulated astrocytes release high-mobility group 1 protein, an inducer of LAN-5 neuroblastoma cell differentiation. Neuroscience **82**:1021–1028.
42. **Sakiyama, H., T. Nonaka, R. Masuda, N. Inoue, Y. Kuboki, M. Iijima, Y. Hirabayasi, M. Takahagi, K. Yoshida, K. Kuriiwa, M. Yoshida, and S. Imajoh-Ohmi.** 2002. Characterization of mineral deposits formed in cultures of a hamster tartrate-resistant acid phosphatase (TRAP) and alkaline phosphatase (ALP) double-positive cell line (CCP). Cell Tissue Res. **309**:269–279.
43. **Salmivirta, M., H. Rauvala, K. Elenius, and M. Jalkanen.** 1992. Neurite growth-promoting protein (amphoterin, p30) binds syndecan. Exp. Cell Res. **200**:444–451.
44. **Sato, T., M. del Carmen Ovejero, P. Hou, A. M. Heegaard, M. Kumegawa, N. T. Foged, and J. M. Delaisse.** 1997. Identification of the membrane-type matrix metalloproteinase MT1-MMP in osteoclasts. J. Cell Sci. **110**(Pt. 5): 589–596.
45. **Scaffidi, P., T. Misteli, and M. E. Bianchi.** 2002. Release of chromatin protein HMGB1 by necrotic cells triggers inflammation. Nature **418**:191–195.
46. **Schlueter, C., H. Weber, B. Meyer, P. Rogalla, K. Roser, S. Hauke, and J. Bullerdiek.** 2005. Angiogenetic signaling through hypoxia: HMGB1: an angiogenetic switch molecule. Am. J. Pathol. **166**:1259–1263.
47. **Stickens, D., D. J. Behonick, N. Ortega, B. Heyer, B. Hartenstein, Y. Yu, A. J. Fosang, M. Schorpp-Kistner, P. Angel, and Z. Werb.** 2004. Altered endochondral bone development in matrix metalloproteinase 13-deficient mice. Development **131**:5883–5895.
48. **Taguchi, A., D. C. Blood, G. del Toro, A. Canet, D. C. Lee, W. Qu, N. Tanji, Y. Lu, E. Lalla, C. Fu, M. A. Hofmann, T. Kislinger, M. Ingram, A. Lu, H. Tanaka, O. Hori, S. Ogawa, D. M. Stern, and A. M. Schmidt.** 2000. Blockade of RAGE-amphoterin signalling suppresses tumour growth and metastases. Nature **405**:354–360.
49. **Takami, M., N. Kim, J. Rho, and Y. Choi.** 2002. Stimulation by Toll-like receptors inhibits osteoclast differentiation. J. Immunol. **169**:1516–1523.
50. **Talreja, J., M. H. Kabir, B. F. M., D. J. Stechschulte, and K. N. Dileepan.** 2004. Histamine induces Toll-like receptor 2 and 4 expression in endothelial cells and enhances sensitivity to gram-positive and gram-negative bacterial cell wall components. Immunology **113**:224–233.
51. **Taniguchi, N., K. Kawahara, K. Yone, T. Hashiguchi, M. Yamakuchi, M. Goto, K. Inoue, S. Yamada, K. Ijiri, S. Matsunaga, T. Nakajima, S. Komiya, and I. Maruyama.** 2003. High mobility group box chromosomal protein 1 plays a role in the pathogenesis of rheumatoid arthritis as a novel cytokine. Arthritis Rheum. **48**:971–981.
52. **Vortkamp, A., K. Lee, B. Lanske, G. V. Segre, H. M. Kronenberg, and C. J. Tabin.** 1996. Regulation of rate of cartilage differentiation by Indian hedgehog and PTH-related protein. Science **273**:613–622.
53. **Vu, T. H., and Z. Werb.** 2000. Matrix metalloproteinases: effectors of development and normal physiology. Genes Dev. **14**:2123–2133.
54. **Wang, H., O. Bloom, M. Zhang, J. M. Vishnubhakat, M. Ombrellino, J. Che, A. Frazier, H. Yang, S. Ivanova, L. Borovikova, K. R. Manogue, E. Faist, E. Abraham, J. Andersson, U. Andersson, P. E. Molina, N. N. Abumrad, A. Sama, and K. J. Tracey.** 1999. HMG-1 as a late mediator of endotoxin lethality in mice. Science **285**:248–251.
55. **Wang, H., H. Yang, and K. J. Tracey.** 2004. Extracellular role of HMGB1 in inflammation and sepsis. J. Intern. Med. **255**:320–331.
56. **Wang, K., H. Yamamoto, J. R. Chin, Z. Werb, and T. H. Vu.** 2004. Epidermal growth factor receptor-deficient mice have delayed primary endochondral ossification because of defective osteoclast recruitment. J. Biol. Chem. **279**: 53848–53856.
57. **Yamada, S., K. Inoue, K. Yakabe, H. Imaizumi, and I. Maruyama.** 2003. High mobility group protein 1 (HMGB1) quantified by ELISA with a monoclonal antibody that does not cross-react with HMGB2. Clin. Chem. **49**: 1535–1537.
58. **Youn, J. H., and J. S. Shin.** 2006. Nucleocytoplasmic shuttling of HMGB1 is regulated by phosphorylation that redirects it toward secretion. J. Immunol. **177**:7889–7897.
59. **Zelzer, E., W. McLean, Y. S. Ng, N. Fukai, A. M. Reginato, S. Lovejoy, P. A. D'Amore, and B. R. Olsen.** 2002. Skeletal defects in VEGF(120/120) mice reveal multiple roles for VEGF in skeletogenesis. Development **129**:1893–1904.
60. **Zhou, Z., D. Immel, C. X. Xi, A. Bierhaus, X. Feng, L. Mei, P. Nawroth, D. M. Stern, and W. C. Xiong.** 2006. Regulation of osteoclast function and bone mass by RAGE. J. Exp. Med. **203**:1067–1080.

ELSEVIER

Cardiovascular Pathology 16 (2007) 136–143

CARDIOVASCULAR PATHOLOGY

Original Article

HMGB1 expression by activated vascular smooth muscle cells in advanced human atherosclerosis plaques☆

Katsumi Inoue[a], Ko-ichi Kawahara[b], Kamal Krishna Biswas[b], Kenji Ando[c], Kazuaki Mitsudo[a], Masakiyo Nobuyoshi[c], Ikuro Maruyama[b,*]

[a]*Department of Cardiology, Kurashiki Central Hospital, Kurashiki, Japan*
[b]*Department of Laboratory and Vascular Medicine, Cardiovascular and Respiratory Disorders, Advanced Therapeutics, Graduate School of Medical and Dental Sciences, Kagoshima University, Kagoshima 890-8520, Japan*
[c]*Department of Cardiology, Kokura Memorial Hospital, Kitakyusyu, Japan*

Received 26 July 2006; received in revised form 26 September 2006; accepted 16 November 2006

Abstract

Background: Chronic inflammation plays a key role in atherogenesis, which is followed by atheromatous plaque instability. High-mobility group box 1 is released by activated macrophages as a late-phase mediator during prolonged inflammation. However, the expression of high-mobility group box 1 and its effect on the production of C-reactive protein and matrix metalloproteinases, particularly on human vascular smooth muscle cells, still remain unknown. **Methods and results:** Immunohistochemical studies revealed that high-mobility group box 1 was abundantly expressed in vascular smooth muscle cells of carotid and coronary atheromatous plaques, but not in atrophic vascular smooth muscle cells of fibrous plaques and normal medial vascular smooth muscle cells. Receptor for advanced glycation end products was also detected in vascular smooth muscle cells positive for high-mobility group box 1. Moreover, vascular smooth muscle cells positive for high-mobility group box 1 were found to express both C-reactive protein and matrix metalloproteinases (2, 3, and 9). Administration of exogenous high-mobility group box 1 to cultured vascular smooth muscle cells caused a marked elevation of C-reactive protein mRNA by reverse transcriptase–polymerase chain reaction and of C-reactive protein levels by enzyme-linked immunosorbent assay. Conversely, C-reactive protein also triggered a significant release of high-mobility group box 1 in vascular smooth muscle cell culture medium as determined by immunoblot. **Conclusions:** Activated vascular smooth muscle cells are the source of high-mobility group box 1 in human advanced atherosclerotic lesions. High-mobility group box 1 directly stimulates the production of both C-reactive protein and matrix metalloproteinase through receptor for advanced glycation end product. These findings provide new evidence that high-mobility group box 1 produced by activated vascular smooth muscle cells may contribute to the progression and vulnerability of human atherosclerotic lesions toward rupture.

Keywords: High-mobility group box 1; Smooth muscle cells; Inflammation; Atherosclerosis; Plaque instability

1. Introduction

High-mobility group box 1 (HMGB1) is a ubiquitous and abundant chromatin component that stabilizes nucleosome structure and enables the bending of DNA, resulting in facilitation of gene transcription [1]. Recently, additional roles of HMGB1—acting as a proinflammatory cytokine and playing a role in inflammation—have been implicated [2]. HMGB1 is secreted by activated macrophages and acts as a late-phase mediator of inflammation and induced

☆ Katsumi Inoue and Ko-ichi Kawahara contributed equally to this work.

This study was supported by research grants from the Ministry of Education, Culture, Sports, Science, and Technology of Japan; Grants-in-Aid 17100007 (to S. Takao) and 18791341 (to T. Ito); and Health and Labor Sciences research grant from the Ministry of Health, Labor, and Welfare (to I. Maruyama).

* Corresponding author. Tel.: +81 99 275 5437; fax: +81 99 275 2629.
E-mail address: rinken@m3.kufm.kagoshima-u.ac.jp (I. Maruyama).

1054-8807/07/$ – see front matter © 2007 Elsevier Inc. All rights reserved.
doi:10.1016/j.carpath.2006.11.006